The stratigraphic signature of the late Cenozoic Antarctic Ice Sheets in the Ross Embayment

Robert McKay[1,†], Greg Browne[2], Lionel Carter[1], Ellen Cowan[3], Gavin Dunbar[1], Lawrence Krissek[4], Tim Naish[1,2], Ross Powell[5], Josh Reed[6], Franco Talarico[7], and Thomas Wilch[8]

[1]*Antarctic Research Centre, Victoria University of Wellington, P.O. Box 600, Wellington, New Zealand*
[2]*GNS Science, P.O. Box 30368, Lower Hutt, New Zealand*
[3]*Department of Geology, Appalachian State University, Boone, North Carolina 28608-2067, USA*
[4]*School of Earth Sciences and Byrd Polar Research Center, Ohio State University, Columbus, Ohio 43210, USA*
[5]*Department of Geology and Environmental Geosciences, Northern Illinois University, DeKalb, Illinois 60115-2854, USA*
[6]*ANDRILL Science Management Office,126 Bessey Hall, University of Nebraska-Lincoln, P.O. Box 88085, Lincoln, Nebraska 68588-0341, USA*
[7]*Università di Siena, Dipartimento di Scienze delle Terra, I-53100 Siena, Italy*
[8]*Department of Geology, Albion College, Albion, Michigan 49224, USA*

ABSTRACT

A 1284.87-m-long sediment core (AND-1B) from beneath the McMurdo sector of the Ross Ice Shelf provides the most complete single section record to date of fluctuations of the Antarctic Ice Sheets over the last 13 Ma. The core contains a succession of subglacial, glacimarine, and marine sediments that comprise ~58 depositional sequences of orbital-scale duration. These cycles are constrained by a chronology based on biostratigraphic, magnetostratigraphic, and $^{40}Ar/^{39}Ar$ isotopic ages. Each sequence represents a record of a grounded ice-sheet advance and retreat cycle over the AND-1B drill site, and all sediments represent subglacial or marine deposystems with no subaerial exposure surfaces or terrestrial deposits. On the basis of characteristic facies within these sequences, and through comparison with sedimentation in modern glacial environments from various climatic and glacial settings, we identify three facies associations or sequence "motifs" that are linked to major changes in ice-sheet volume, glacial thermal regime, and climate. Motif 1 is documented in the late Pleistocene and in the late Middle Miocene intervals of AND-1B, and it is dominated by diamictite of subglacial origin overlain by thin mudstones interpreted as ice-shelf deposits. Motif 1 sequences lack evidence of subglacial meltwater and represent glaciation under cold, "polar"-type conditions. Motif 2 sequences were deposited during the Pliocene and early Pleistocene section of AND-1B and are characterized by subglacial diamictite overlain by a relatively thin proglacial-marine succession of mudstone-rich facies deposited during glacial retreat. Glacial minima are represented by diatom-bearing mudstone, and diatomite. Motif 2 represents glacial retreat and advance under a "subpolar" to "polar" style of glaciation that was warmer than present, but that had limited amounts of subglacial meltwater. Motif 3 consists of subglacial diamictite that grades upward into a 5- to 10-m-thick proglacial retreat succession of stratified diamictite, graded conglomerate and sandstone, graded sandstone, and/or rhythmically stratified mudstone. Thick mudstone intervals, rather than diatomite-dominated deposition during glacial minima, suggest increased input of meltwater from nearby terrestrial sources during glacial minima. Motif 3 represents Late Miocene "subpolar"-style glaciation with significant volumes of glacially derived meltwater.

INTRODUCTION

The history of the Antarctic ice sheets through the Cenozoic remains poorly known due to Antarctica's remoteness and ice cover for the last 34 Ma. Direct physical records of Antarctic Cenozoic glacial history have become available only recently, and those largely from offshore shelf basins through seismic surveys (e.g., De Santis et al., 1999; Bart et al., 2000) and geological drilling programs (e.g., Ocean Drilling Program [ODP], Cape Roberts Project [CRP], SHALDRIL, and ANDRILL; Naish et al., 2008). The number of sites drilled is small, and they are mainly confined to three areas: McMurdo Sound (e.g., Barrett, 1989, 2007), Prydz Bay (e.g., Barron et al., 1989; Shipboard Scientific Party, 2001), and the Antarctic Peninsula (e.g., Barker et al., 1999). Even in McMurdo Sound, where Oligocene and Lower Miocene strata are well-documented (Naish et al., 2001), research has focused on the evolution and early history of the larger East Antarctic Ice Sheet, whereas the mid-Miocene to Quaternary history of both the East and West Antarctic Ice Sheets remains largely unknown and poorly dated.

The $\delta^{18}O$ record from benthic foraminifera implies a profound cooling ca. 14 Ma, interpreted as an expansion of the East Antarctic Ice Sheet to perhaps its present-day extent (e.g., Zachos et al., 2001). Several lines of evidence, including geomorphologic studies from the Transantarctic Mountains (Sugden et al., 1993), have suggested that East Antarctic Ice Sheet has been more or less stable and cold for the last ~14 Ma. This is based largely on $^{40}Ar/^{39}Ar$ tephrochronology from the Dry Valleys region, which places a shift from "wet-based" terrestrial glaciation to less dynamic, "cold-based" terrestrial glaciation at ca. 15–13 Ma (e.g., Sugden et al., 1993; Lewis et al., 2006, 2007). Despite this evidence for a stepwise shift in climate and glacial regime, deep-ocean oxygen isotope records indicate that moderate oscillations of global ice volume continued until the development of Northern Hemisphere ice

†E-mail: robert.mckay@vuw.ac.nz.

GSA Bulletin; November/December 2009; v. 121; no. 11/12; p. 1537–1561; doi: 10.1130/B26540.1; 12 figures; 2 tables.

sheets ca. 3 Ma (e.g., Raymo, 1994). These oscillations are thought to have involved ice volume changes on Greenland, the marine-based West Antarctic Ice Sheet, and, at times, the margins of the East Antarctic Ice Sheet capable of producing global sea-level fluctuations of up to 25 m (Kennett and Hodell, 1993).

The occurrences of Pliocene-age marine diatoms in the *Nothofagus*-bearing tills of the Sirius Group at a number of locations high in the Transantarctic Mountains led Webb et al. (1984) to propose that diatomaceous sediments had been deposited in interior seas in East Antarctica, and that they were subsequently glacially eroded and transported to their present sites. This concept requires one or more significant deglaciations of East Antarctica, and wet-based (subpolar to temperate) glaciation suggested until ca. 3 Ma. CIROS-2, a sediment drill core collected at the mouth of Ferrar Fjord, McMurdo Sound, recovered a discontinuous record of this critical Pliocene-to-Pleistocene interval. The Pleistocene section of CIROS-2 contains interbedded subglacial and glaciolacustrine facies that are thought to indicate periods of Ferrar Glacier expansion (recorded by the subglacial facies) alternating with periods of ice-sheet expansion in the Ross Embayment. This expansion is interpreted to have dammed a deglaciated Ferrar Fjord, as recorded by glaciolacustrine facies (Barrett and Hambrey, 1992). The Pliocene section of CIROS-2 is dominated by diamictite facies, which are interpreted as subglacial deposits of an expanded Ferrar Glacier (an East Antarctic Ice Sheet outlet glacier) with periods of ice expansion from the Ross Embayment (Sandroni and Talarico, 2006). Although these diamictites are interstratified with glacimarine muds, there is no evidence of substantial volumes of subglacial meltwater, suggesting that during the Pliocene, the glacial regime was not much warmer than the present day (Barrett and Hambrey, 1992).

Although uncertainty remains about the scale of East Antarctic Ice Sheet dynamism (e.g., Webb and Harwood, 1991; Sugden et al., 1993), the early to middle Pliocene (5–3 Ma) generally is regarded as a time of relative global warmth (e.g., Crowley et al., 1996), and an important window into Earth's future climate if projections of anthropogenic global warming (IPCC, 2007) are correct.

The Neogene and Quaternary evolution and stability of the marine-based Antarctic Ice Sheet in the Ross Embayment is poorly documented, although its behavior since the Last Glacial Maximum (ca. 18,000 yr B.P.) is moderately well-constrained (Conway et al., 1999; Domack et al., 1999; McKay et al., 2008). Since the Last Glacial Maximum, ice cover in the Ross and Ronne-Filchner Embayments has shifted from ice sheets that expanded to near the continental shelf edge to large floating ice shelves (Shipp et al., 1999; Licht et al., 1999). However, the response of this marine-based ice-sheet system to late Quaternary orbital cycles remains unclear. Scherer et al. (1998) provided evidence that parts of the West Antarctic Ice Sheet that are now grounded actually collapsed at least once during the late Pleistocene, based on marine diatoms recovered from beneath Ice Stream B. The potential collapse of the West Antarctic Ice Sheet during the late Pleistocene is also partially supported by modeling studies suggesting that West Antarctic Ice Sheet collapse may be irregularly timed with respect to orbital forcing parameters, and that the distribution of soft, deformable till underlying the West Antarctic Ice Sheet may be critical in determining its stability (MacAyeal, 1992).

Marine sediments from Deep Sea Drilling Program (DSDP) Site 270 indicate that continental glaciation extended onto the Ross Sea continental shelf episodically since at least the late Oligocene (Hayes et al., 1975; Leckie and Webb, 1983; Bart et al., 2000). To date, no well-constrained and detailed physical record of past oscillations of the marine-based ice sheets that occupied the Ross Embayment has been available to test these hypotheses. Continuous seismic units and erosional surfaces indicate that major ice-sheet expansions occurred across the Ross Sea continental shelf during the mid-Miocene between ca. 16.5 and 10 Ma, and a major unconformity at ca. 10 Ma is interpreted as representing the development of a "temperate" to "subpolar" ice sheet (De Santis et al., 1995). Seismic profiles also indicate that ice streams, derived from the East Antarctic Ice Sheet, expanded into the northwestern sector of the Ross Sea on at least eight occasions since the late Neogene. Large unconformities in seismic profiles from the eastern Ross Sea suggest that West Antarctic Ice Sheet expansion across the Ross Sea continental shelf occurred as early as the middle Miocene (Bart et al., 2000; Bart, 2003). Widespread expansion of the West Antarctic Ice Sheet at this time requires either a shallower Ross Sea or cold glacial regime in order to support the development of an ice sheet across the Ross Embayment that is grounded below sea level. Overdeepening of the continental shelf during the mid-Miocene is thought to have been sufficient enough to prevent subaerial exposures on the bathymetric highs in the Ross Sea since this time (Brancolini et al., 1995). Seismic records from Bart (2001) indicate that ice sheets were periodically advancing onto the continental shelves around the Antarctic margin during the early Pliocene, despite evidence for warmer-than-present temperatures during the early Pliocene (Kennett and Hodell, 1993). Recent results from the ANDRILL Program AND-1B drill core, integrated with a new ice sheet model, imply a dynamic WAIS oscillating in volume by up to +5 m sea level equivalent in response to 40-ka obliquity cycles (Naish et al., 2009).

The ANDRILL McMurdo Ice Shelf Project

In the austral summer of 2006–2007, the McMurdo Ice Shelf project of the ANtarctic Geological DRILLing program (ANDRILL) successfully cored a 1284.87-m-long record of climate and glacial/marine history spanning the last 13 Ma. The core (AND-1B) was recovered from beneath the northwestern corner of the Ross Ice Shelf (Fig. 1; Naish et al., 2008), referred to as the McMurdo Ice Shelf (77.89°S, 167.09°E), and it contains ~58 sequences recording advance and retreat of a grounded ice margin (Fig. 2). Ice-shelf thickness at the drill site presently is ~82 m, and water depth is ~835 m. This unique core represents the most complete single record to date of past ice-sheet oscillations, and a range of lithofacies can accurately identify periods of glacial advance and retreat within the Ross Embayment.

In this paper, we present the lithofacies scheme for AND-1B and use it to track changes in glacial and marine depositional environments as recorded in AND-1B. Three vertical facies successions (Fig. 2), or "motifs," occur repeatedly in AND-1B. These "motifs" are defined and related to glacial-interglacial oscillations of the grounding line under three different styles of glaciation, or thermal regimes, for the late Cenozoic ice sheets. Based on data from AND-1B and previous drill cores from McMurdo Sound, we present a depositional model for each "motif" that accounts for ice-sheet grounding-line oscillations, the influence of local East Antarctic Ice Sheet outlet glaciers, and coastal processes in the western Ross Sea.

PREVIOUS HIGH-LATITUDE GLACIMARINE DEPOSITIONAL MODELS

The interpretations of past glacial regimes made in this paper are based on modern analogs of sedimentation in subpolar (e.g., Greenland/Spitsbergen) and polar (e.g., Antarctica) glacial environments (see Table 1). The use of "wet(warm)-based" or "dry(cold)-based" is somewhat ambiguous in the context of interpreting past glacimarine sedimentation, since the present-day Antarctic Ice Sheet is now known to contain a significant subglacial drainage network (Siegert et al., 2005; Wingham et al., 2006; Fricker et al., 2007), and, therefore, there

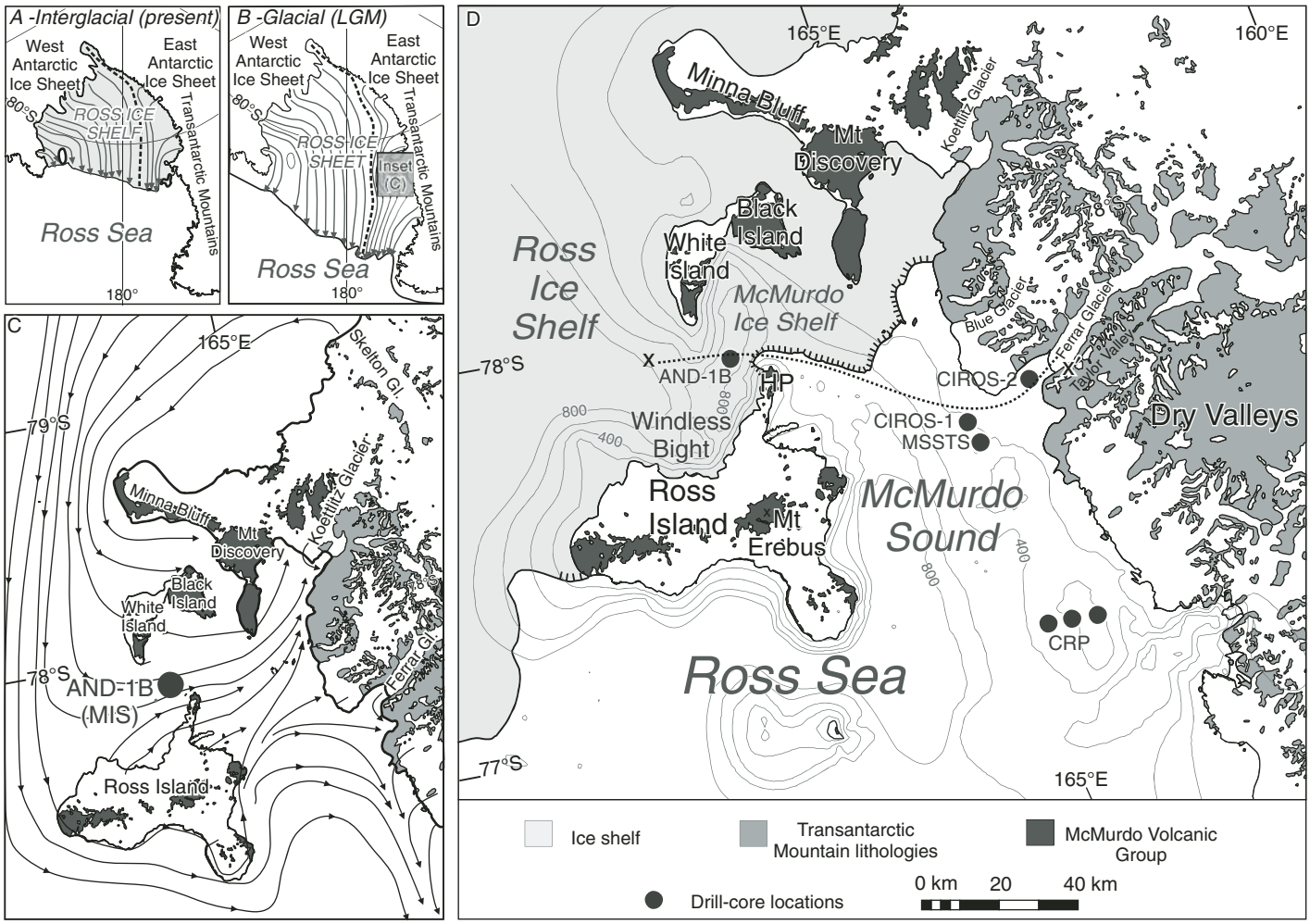

Figure 1. Ice flow-line pathways for (A) the present-day Ross ice shelf showing West Antarctic Ice Sheet versus East Antarctic Ice Sheet contributions (after Fahnestock et al., 2000) and (B) a reconstruction of the grounded ice sheet in the Ross Embayment at Last Glacial Maximum (LGM), showing the West Antarctic Ice Sheet versus East Antarctic Ice Sheet contribution (after Denton and Hughes, 2002). (C) A high-resolution inset of LGM flow-line reconstruction for the McMurdo Sound Region based on geological and geomorphic evidence (after Denton and Hughes, 2002). This shows the pathway for ice originating from the southern Transantarctic Mountains outlet glaciers into Windless Bight during periods of glacial expansion and grounded ice. (D) McMurdo Sound region and the AND-1B drill site near Hut Point (HP), as well as previous drill cores (MSSTS, CIROS, CRP) collected in the region. Transect x-x′ shows approximate cross section for sedimentation model cartoons (Figs. 10–12).

is some potential for deposition by "wet-based" ice in the modern Antarctic environment. Previous work on sedimentary models, as well as process studies from high-latitude continental shelf settings, has identified stratigraphic subdivisions and sedimentary characteristics for different glacial thermal regimes (i.e., polar, subpolar, and temperate; see Table 1) that are dependent on climatic setting, local physiography/oceanography, and glacial processes (e.g., Anderson and Ashley, 1991; Powell and Molnia, 1989; Powell and Domack, 2002; Dowdeswell et al., 1998; Ó Cofaigh et al., 2001; Ó Cofaigh and Dowdeswell, 2001; Desloges et al., 2002).

Domack et al. (1999, 2005) and McKay et al. (2008) documented late Quaternary sedimentation associated with the cold "polar" glacial regime of the West Antarctic Ice Sheet and East Antarctic Ice Sheet, the coldest end member for present-day glacimarine deposition (see Table 1), with no significant surface melt and limited subglacial meltwater influence. Processes associated with this glacial regime produce low (<0.05 mm/a) terrigenous sedimentation rates in the glacimarine–ice-shelf environment relative to higher biogenic sedimentation rates (>0.2 mm/a) in nearby open marine environments, including the immediate vicinity of ice-shelf calving lines. These studies examined sedimentary processes associated with the transition from a grounded ice sheet to open-marine environments in continental shelf basins within the Ross Sea (including under the McMurdo Ice Shelf) since the Last Glacial Maximum. They identified a facies succession that consists of, in ascending stratigraphic order:

(1) massive mud-rich diamict(ite), interpreted as subglacial till deposited beneath grounded ice;
(2) stratified diamict(ite) with a sandy mud component, interpreted as a basal debris meltout zone associated with lift-off and development of a floating ice shelf;
(3) sparsely fossiliferous (<10% biosiliceous, mostly reworked diatom frustules) and non-bioturbated mud(stone) lacking lonestones, interpreted as a sub–ice-shelf facies; and

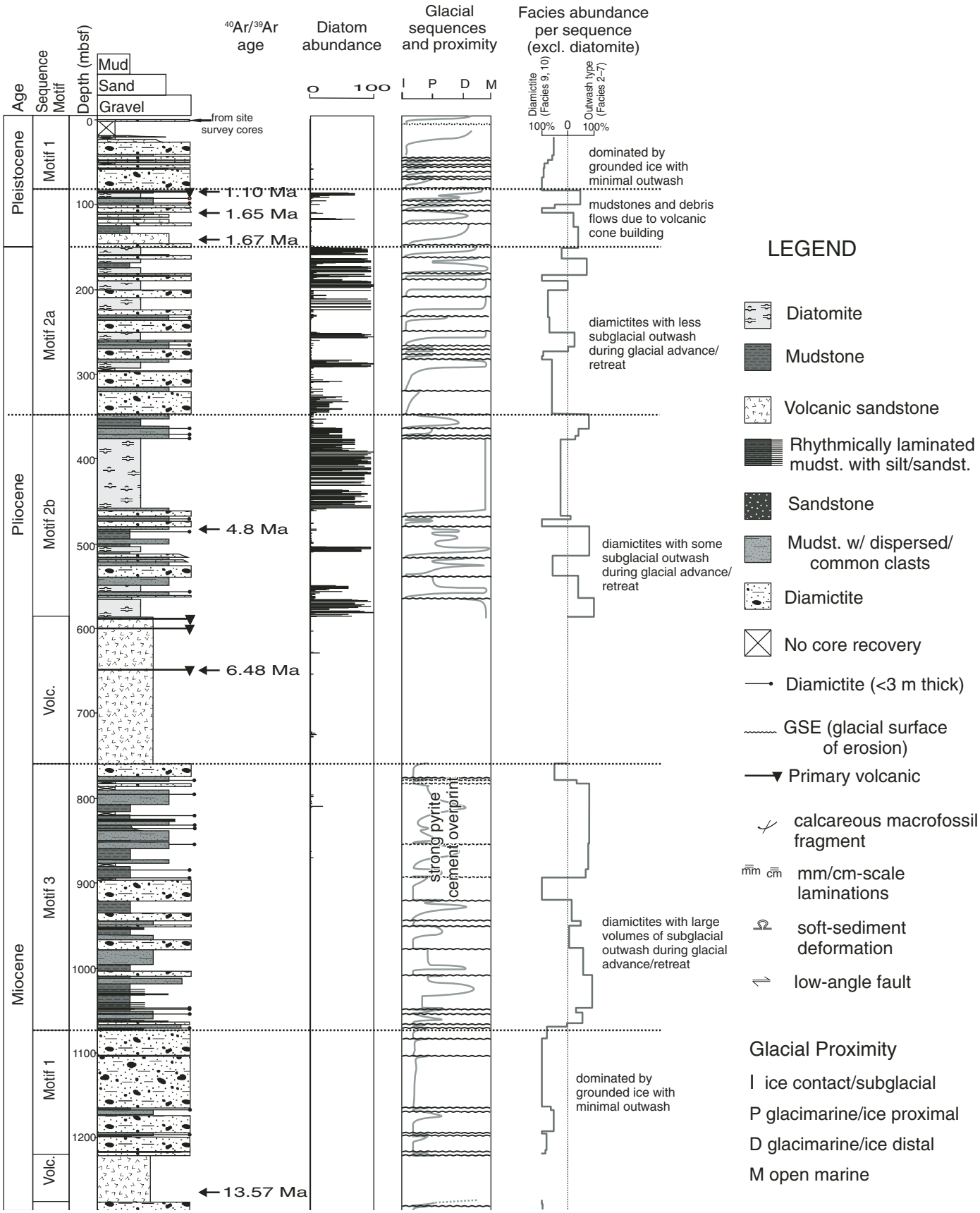

Figure 2.

Figure 2. Stratigraphic log and interpretation of AND-1B core. Age intervals are based on the initial age model of Wilson et al. (2007). Diatom abundance histogram is based on visual estimates from smear slides. Facies abundance curve measures the relative abundance of diamictite facies (facies 9, 10) versus mudstone-rich and/or "outwash type" facies (facies 2, 3, 4, 5, 6, 7) within each sequence. The glacial proximity curve was determined using the models presented in Figures 10–12. Glacial surfaces of erosion (GSEs) define each sequence boundary.

(4) diatom-bearing to diatom-rich (i.e., 10%–50% diatomaceous) mud(stone) and diatom(ite) ooze (>50% diatomaceous) with lonestones, indicative of open-marine conditions and iceberg rafting.

Lowe and Anderson (2002) recovered sediments cores with some evidence of meltwater discharge from near the terminus of the Pine Island Glacier in West Antarctica, although these meltwater facies were restricted to mudstones generally <1 m, but up to 4.5 m thick, with rare deposits of sandstone and gravels. This highlights that even in a cold polar glacial regime, some subglacial meltwater may be present. However, the spatial (and temporal) distribution of subglacial meltwater discharge appears to be rare and highly restricted— in this case, to the terminus of the third largest drainage outlet in West Antarctica. Geophysical studies of the seafloor geomorphology of the Ross Sea continental shelf indicate that subglacial meltwater discharge associated with the retreat of Last Glacial Maximum ice sheet in the Ross Embayment was rare and spatially restricted (Shipp et al., 1999; McMullen et al., 2006).

"Temperate" glaciers (i.e., those at the pressure melting point throughout) represent the warmest end member for glacimarine sedimentation, and they are characterized by large meltwater plumes and high sediment load. Terrigenous sedimentation rates are several orders of magnitude higher (e.g., 2–20 m/a in ice-proximal setting; 0.14 m/a, 15 km from the grounding line) than their polar glacimarine counterparts, diluting and/or suppressing the biogenic component to a few percent (Cowan and Powell, 1991; Cowan et al., 1997; Powell and Domack, 2002). Graded laminae and rhythmic bedding with iceberg-rafted debris are characteristic of glacimarine sedimentation under a temperate glacial regime, due to the abundance of meltwater and large fan systems that form at the grounding line (Cowan et al., 1999; Powell, 1990).

"Subpolar" glacimarine deposition is more difficult to characterize because it represents an intermediate phase between temperate and polar glaciation. Therefore, glacimarine sedimentation under a subpolar regime varies widely in response to the extent of surface and subglacial melting and/or iceberg influences, even in similar climatic settings (see Table 1). In modern glacial environments, an increase in subglacial meltwater is likely to produce a higher terrigenous sedimentation rate during grounding line retreat/advance (Table 1). Deposition of rhythmically laminated sediments and outwash facies, such as sands and conglomerates, is also more likely in a meltwater-dominated regime, but these facies have also been documented in the colder end members of subpolar environments, such as East Greenland (Dowdeswell et al., 1998; Ó Cofaigh et al., 2001; Ó Cofaigh and Dowdeswell, 2001). An additional complication is that the extent of subglacial meltwater discharge is also likely to be spatially variable along the grounding line (Powell, 1990).

The three "motifs" that we define here for AND-1B are used to further enhance sequence stratigraphic models of high-latitude continental margins, as well as to provide insight into the late Cenozoic evolution of the Antarctic Ice Sheets. These "motifs" represent a continuum of glacial regime, from a system dominated by cold polar-style glaciation (similar to today) during the early part of the Late Miocene, to a warmer regime with abundant subglacial meltwater discharge during the Pliocene, and back into the present-day style of cold polar-style glacimarine sedimentation during the Pleistocene. The stratigraphic architecture of the motifs is entirely controlled by variations in the position of the grounding/calving lines as they have accumulated sediment in deep water, below the direct influence of the wave-base and sea-level fluctuations.

GEOLOGICAL SETTING

AND-1B was drilled in the southern portion of the Victoria Land Basin (Fig. 1), one of three major north-south–trending sedimentary basins that form the West Antarctic Rift System. The drill hole is located on the western margin of Victoria Land Basin within the Terror Rift, a 70-km-wide structure extending from Mount Erebus in the south to Mount Melbourne, ~350 km to the north (e.g., Cooper et al., 1987). Within McMurdo Sound, the Terror Rift contains ~3.5 km of sediments, accumulated along its central axis since the middle Miocene (Henrys et al., 2007). Sediment in the western Ross Sea today is accumulating primarily in the north-south–trending basin troughs between 600 and 1200 m deep. These troughs are thought to be the sites of former ice streams that drained outlet glaciers of the West and East Antarctic Ice Sheets during the Last Glacial Maximum (Hughes, 1977; Denton and Hughes, 2000; Mosola and Anderson, 2006). The AND-1B drill site is situated within an ~900-m-deep basin that surrounds most of Ross Island. Termed a "flexural moat," this basin is believed to have formed through a combination of localized lithospheric loading caused by the development of Ross Island's volcanoes, beginning around 4.6 Ma, superimposed on the regional pattern of rift subsidence (Stern et al., 1991; Horgan et al., 2005). These volcanic emergences include Mount Bird at ca. 4.6 Ma (Wright and Kyle, 1990a), Mount Terror at ca. 1.75 Ma (Wright and Kyle, 1990b), and Hut Point Peninsula and Mount Erebus at ca. 1.3 Ma (Esser et al., 2004). White Island dates back to 7.65 Ma, but its northern margin is as young as 0.17 Ma (Cooper et al., 2007).

GLACIAL SETTING AND CONTEXT

AND-1B was drilled at Windless Bight beneath the McMurdo Ice Shelf (Fig. 1), which is considered to be an extension of the Ross Ice Shelf at its northwest margin. The McMurdo ice shelf has a surface snow accumulation of ~0.3 m/a (McCrae, 1984), and the present-day calving line is ~5 km from the drill site. Basal melting of the ice shelf is currently occurring at the AND-1B drill site, but the ice is likely free of sediment (McCrae, 1984; Barrett et al., 2005). The Ross Ice Shelf itself is a major component of the West Antarctic Ice Sheet system, and approximately two-thirds of the ice shelf is nourished by ice streams that drain the West Antarctic Ice Sheet, yet its western margin is fed by East Antarctic Ice Sheet outlet glaciers (Fahnestock et al., 2000; Fig. 1). Glaciological reconstructions of grounded ice expansion within the Ross Embayment during the Last Glacial Maximum (Denton and Hughes, 2000) indicate that an ice sheet extended to near the edge of the continental shelf and was fed by contributions from both East and West Antarctica (Fig. 1), although uncertainty over the exact contribution from each source during the Last Glacial Maximum remains (e.g., Licht et al., 2005).

We interpret the glacimarine cycles in AND-1B as documenting retreat and advance of a large marine-based ice sheet within the Ross Embayment. This ice sheet was susceptible

TABLE 1. EXAMPLES OF MODERN (POST-LGM) ANALOGS FROM VARIOUS GLACIAL THERMAL REGIMES

AND-1B interpretation	Glacial regime	Type example	Grounding line proximity	Subglacial/marine conditions	Characteristic glacimarine sedimentary processes	Characteristic lithofacies	Climatic setting	References
Mode 1	Polar	Ross Embayment, Antarctica (large and fringing ice shelves)	Proximal	Basal melting rate of Ross Ice Shelf at grounding line <4 m/a to >40 m/a. Subglacial meltwater discharging from Siple Coast grounding line is unknown but appears to have been rare and localized during LGM retreat. Transantarctic Mountains (TAM) outlet glacier (MacKay Glacier) basal melting rate is 1.7 m/a, with no conduit flow observed. Suspended particulate matter (SPM) beneath Ross Ice Shelf, ~100 km from grounding line (site J9) is 0.68 mg/L. SPM up to 14 mg/L within 5 km of MacKay Glacier grounding line.	Subglacial till deformation and lodgment. Melt-out of debris entrained in basal ice expected close to grounding ± sediment gravity flows. Subglacial till accumulation rate is 4.1 mm/a at Mackay Glacier. Proximal glacimarine accumulation rate is 5.5 mm/a at Mackay Glacier. Tidal pumping of grounding zone. Slope instability after grounding line retreat.	Massive diamicton (subglacial till) beneath present-day, grounded West Antarctic Ice Sheet (WAIS) ice streams. Overthickening of subglacial till packages in grounding zone wedges during stillstands. Massive or stratified diamicton (meltout of basal debris and debris flows near grounding line). Strong to weakly (noncyclic) laminated muds with occasional sand beds and minor biosiliceous component.	Mean annual temp. (McMurdo) –17 °C Mean summer temp. (McMurdo) –3 °C Sub–ice-shelf water temp. –2 °C	Carter et al. (1981) MacPherson (1987) Powell et al. (1996) Dawber and Powell (1997) Tulaczyk et al. (1998) Domack et al. (1999) Rignot and Jacobs (2002) McKay et al. (2008)
			Distal	Basal melting rate of ice shelves near calving line is estimated at 0.4 m/a but is usually lacking sediment. Open-marine environment with high biogenic productivity and iceberg calving. SPM at McMurdo Ice Shelf edge <5 mg/L (includes biogenic component)	Suspension settling of fine particles advected from open water under the ice shelf ± sediment gravity flows. If ice shelf is narrow and fringing, epibenthic communities may occur. Sediment accumulation rates are ≤0.05 mm/a beneath McMurdo Ice Shelf. Biogenic sedimentation dominates in open water (sed. rate ≤ 0.2 mm/a).	Weakly laminated muds with occasional sand beds and minor reworked biosiliceous component (debris-free ice shelf). Biosiliceous ooze with iceberg-rafted debris (open-marine environment). Local bioturbation and macrofossils if ice shelf is fringing.		
Mode 2a	Polar to Subpolar (iceberg dominated)	Western Antarctic Peninsula (fringing ice shelf or tidewater cliffs)	Proximal	Ice-front melting and iceberg calving. Some subglacial meltwater discharge. SPM generally 8–15 mg/L, but rare meltwater generated surface plumes up to 35 mg/L. Meltwater discharge is spatially variable.	Englacial debris released by ice front melting. Melting of basal debris from calved icebergs. Sediment accumulation rate ~3 mm/a (250 m from grounding line).	Massive or stratified diamicton (meltout of basal debris near grounding line). Sandy muds to muddy sands. Sand laminae common.	Mean annual temp. –3 °C Mean summer temp. 2 °C Sea-surface temp. –1 to 1.6 °C	Domack and Williams (1990) Domack and Ishman (1993) Ashley and Smith (2000) Powell and Domack (2002) Domack et al. (2001)
			Distal	At distances >5 km from grounding line: SPM higher in surface layer of water colum due to phytoplankton blooms. SPM below 50 m water depth is <2 mg/L.	Biogenic dominated sedimentation with sed. rate up to 2 mm/a (due to high productivity and sediment focusing).	Diatomaceous ooze and biosiliceous pebbly muds (contains iceberg-rafted debris) common at distances >5 km from grounding line.		
Mode 2b	Subpolar (iceberg dominated, some meltwater influence)	East Greenland (fjord–tidewater cliff)	Proximal	Meltwater production varies between fjords. Icebergs dominate some E. Greenland fjords (e.g., Scoresby Sund), others are dominated by meltwater production (e.g., Kejser Franz Joseph Fjord [KFJ]). SPM at head of Kangerlussuaq fjord (iceberg dominated) is ~2 mg/L.	Meltwater process can dominate iceberg sedimentation, even in iceberg-dominated fjord. Sed. rate in Kangerlussuaq is 24 mm/a at head of fjord.	Massive or stratified diamicton (meltout of basal debris near grounding line + iceberg scouring). Stratified (including cyclopels/cyclopsams) and massive nonbioturbated muds with dispersed clasts dominate inner KJF Fjord and Scoresby Sund. Sediment gravity flows also common.	Mean annual temp. –7.6 °C Mean summer temp. 2.6 °C Sea-surface temp. –1 to 3 °C	Dowdeswell et al. (1994) Syvitski et al. (1996) Azetsu-Scott and Syvitski (1999) Evans et al. (2002) Ó Cofaigh et al. (2001)
			Distal	Icebergs dominate outer Scoresby Sund. Meltwater production dominates in KFJ. SPM in mouth of Kangerlussuaq fjord <0.5 mg/L.	Iceberg rafting and scouring dominates outer fjords in Scoresby Sund. Meltwater plumes dominate in outer KFJ Fjord and continental shelf with sed. rate ~ 1.1 mm/a. Sedimentation rate in Kangerlussuaq is 0.6 mm/a at mouth of fjord.	Massive diamicton deposited in iceberg-dominated Scoresby Sund. Ice recession from inner shelf to outer mid-KFJ fjord is marked by change from laminated mud to bioturbated mud.		
Mode 3	Subpolar (meltwater dominated)	Spitsbergen (fjord with tidewater cliffs)	Proximal	Meltwater dominated. Icebergs contribute 1–8 mm/a to sediment accumulation rate. SPM up to 300–500 mg/L in Konsfjord.	Basal debris deposited close to grounding line. Settling of mud and rare sand from meltwater plumes dominates near ice front. Sediment accumulation rate of 100 mm/a near ice front in Kongsfjord.	Massive or stratified diamicton (meltout of basal debris near grounding line). Fine-grained muds with layers or lenses of sand/pebbles (iceberg-rafted debris) and cyclopels/cyclopsams. Sand laminae and gravels common within 1 km of ice front (sed. gravity flows).	Mean annual temp. –6.4 °C Mean summer temp. 5.1 °C Sea-surface temp. –1 to 3 °C	Dowdeswell et al. (1998) Dowdeswell and Dowdeswell (1989) Elverhøi et al. (1980, 1983)
			Distal	Meltwater dominated (icebergs contribute 1–8 mm/a to sedimentation rate). SPM values of 1–5 mg/L (5–15 km from grounding line) in Kongsfjord.	Setting of mud from meltwater plumes still dominates 10 km from ice front. Sedimentation accumulation rate of 1 mm/a, 10 km from ice front.	Fine-grained muds with an increase in bioturbation relative to ice-proximal deposits (due to lower sedimentation rate).		

to large variations in spatial extent through glacial-interglacial cycles. The provenance of clasts within subglacially deposited diamictites in the AND-1B record is consistent with transport by glacial ice from East Antarctic Ice Sheet outlet glaciers to the south of the drill site (Pompilio et al., 2007; Talarico and Sandroni, 2007), indicating that grounded ice events in AND-1B were the result of a large-scale advance of the ice sheet across the Ross Embayment, rather than localized glacial advance from Ross Island or outlet glaciers in the McMurdo Sound region.

Ice sheets that occupied the Ross Embayment during past glacial maxima were separated from the land-based sector of the East Antarctic Ice Sheet by the Transantarctic Mountains, but they were linked by large outlet glaciers (Fig. 1). Therefore, the marine-based ice sheets in the Ross Embayment would have had significantly different mass balance controls and responses to past warm periods than the land-based sector of the East Antarctic Ice Sheet. Subglacial sediments in AND-1B were deposited by an ice sheet that was grounded well below sea level and was likely to be highly responsive to oceanographic-related mass balance controls, such as eustasy, iceberg calving, and sub-ice shelf melting. One factor of critical importance with regard to ice-sheet retreat within the greater Ross Embayment (including sections of the presently grounded West Antarctic Ice Sheet) is that marine ice-sheet grounding lines are inherently unstable on reverse bedslopes (Weertman, 1974; Thomas and Bentley, 1978; Schoof, 2007). When combined with an overdeepened bed, forcing factors such as rising sea levels, decreased accumulation rates, increased ice-sheet temperature profile, or decreased basal friction/bed strength may result in the marine ice sheet being forced into an irreversible retreat. This implies that once retreat was initiated for past configurations of the ice sheet in the Ross Embayment, it was likely to occur across the entire embayment, similar to the pattern of retreat documented for the last deglaciation (e.g., Conway et al., 1999; Denton and Hughes, 2002; Licht et al., 1999; Domack et al., 1999; Shipp et al., 1999). Therefore on a glacial-interglacial time scale, the record in AND-1B of advance and retreat of the ice sheets in the Ross Embayment is likely to be intimately tied to the overall state of the West Antarctic Ice Sheet. This interpretation is supported by a new numerical model that incorporates realistic marine grounding line dynamics and demonstrates that retreat of the West Antarctic Ice Sheet was likely to be rapid and occur across the Ross Embayment as a whole (Pollard and De Conto, 2009). The AND-1B record documents past changes, not only in the extent of the marine-based ice sheet in the Ross Embayment over the past 13 Ma, but it also provides insight into changes in the ice-sheet temperature profile (i.e., thermal regime) and basal slipperiness (i.e., basal meltwater).

LITHOFACIES AND IDENTIFICATION OF SUBGLACIAL-GLACIMARINE DEPOSITION IN AND-1B

AND-1B was described at the Crary Science and Engineering Centre, in McMurdo Station, Antarctica, using standard sedimentological techniques to produce detailed stratigraphic logs (Fig. 2; Krissek et al., 2007). From the initial descriptions, 11 lithofacies were defined in the core (Table 2). Lithofacies range from open-marine diatomites, mudstones, and turbidites deposited during interglacials to ice-proximal diamictites, conglomerates, and sandstones deposited during glacial periods. There is no evidence of beach-face facies or facies that contain diagnostic water-depth indicators within AND-1B, suggesting that deposition occurred below storm wave base throughout its deposition. Next, we provide a brief interpretation of the lithofacies critical to the determination of subglacial deposition and glacimarine sedimentary processes. These are used to develop sedimentary models to provide a tool to distinguish past glacial regimes and extent. Detailed descriptions and interpretations of each facies are provided in appendices.

Identifying Subglacial Deposition in AND-1B

Although the genetic origin of diamictites may be highly variable within AND-1B, we identified subglacial and ice-proximal deposition using a range of criteria. Massive and stratified diamictite deposits commonly contain a clast assemblage consistent with a provenance from Transantarctic Mountain outlets (i.e., Skelton and Mulock Glaciers) to the south of the drill site, which indicates transport by distally originating ice rather than deposition by a local ice cap or from outlet glaciers in the McMurdo Sound region (Figs. 3–6; Pompilio et al., 2007; Talarico and Sandroni, 2007). While this is not evidence in itself for subglacial or proximal glacimarine deposition, these diamictites commonly overlie deformed or brecciated glacimarine or open-marine lithofacies. The contact is also often highly sheared or contains clastic intrusions. Above the contact, the diamictite is intermixed with the underlying facies before grading upward into a massive diamictite (e.g., Figs. 7 and 8) that is interpreted to be the result of homogenization by subglacial shearing. The basal characteristics of these diamictites are consistent with known examples of subglacial deposition and overriding by grounded ice (Hart and Boulton, 1991; Hart, 1995). Textural analysis of each facies was untaken by sieve and Sedigraph™, and the diamictites have a homogeneous grain-size distribution (e.g., Figs. 3–6)

TABLE 2. SUMMARY OF LITHOFACIES DOCUMENTED IN THE CORE AND PERCENTAGE OF FACIES THAT CONTRIBUTE TO EACH MOTIF

Facies number and name	Predominant process and interpretation	Motif 1 (%)	Motif 2 (%)	Motif 3 (%)
1. Diatomite	Pelagic rain ± hemipelagic suspension settling	0	37	0
2. Mudstone	Hemipelagic suspension settling	1	8	22
3. Interstratified mudstone and sandstone	Low- to moderate-density sediment gravity flow Hemipelagic suspension settling ±iceberg-rafted debris Redeposition by marine outwash	2	6	10
4. Mudstone with dispersed and/or common clasts	Subglacial deposition Hemipelagic suspension settling Rainout from ice rafting	4	11	29
5. Rhythmically interlaminated mudstone with siltstone or sandstone	Suspension settling from turbid plumes Low-density turbidity current deposition Rainout from ice rafting	0.3	0.2	6
6. Sandstone	Sediment gravity flow	0	2	3
7. Conglomerate	Redeposition by marine outwash Redeposition by mass flow	0.7	0	2
8. Breccia	Sediment redeposition by mass flow. Volcanic debris flow.	0	0.5	0.1
9. Stratified diamictite	Subglacial deposition Rainout with currents Debris-flow deposition	24	3	3
10. Massive diamictite	Subglacial deposition Rainout without currents Debris-flow deposition	68	31	26
11. Volcanic sediment	Primary volcanic deposits/volcanic debris flows	0	1	0

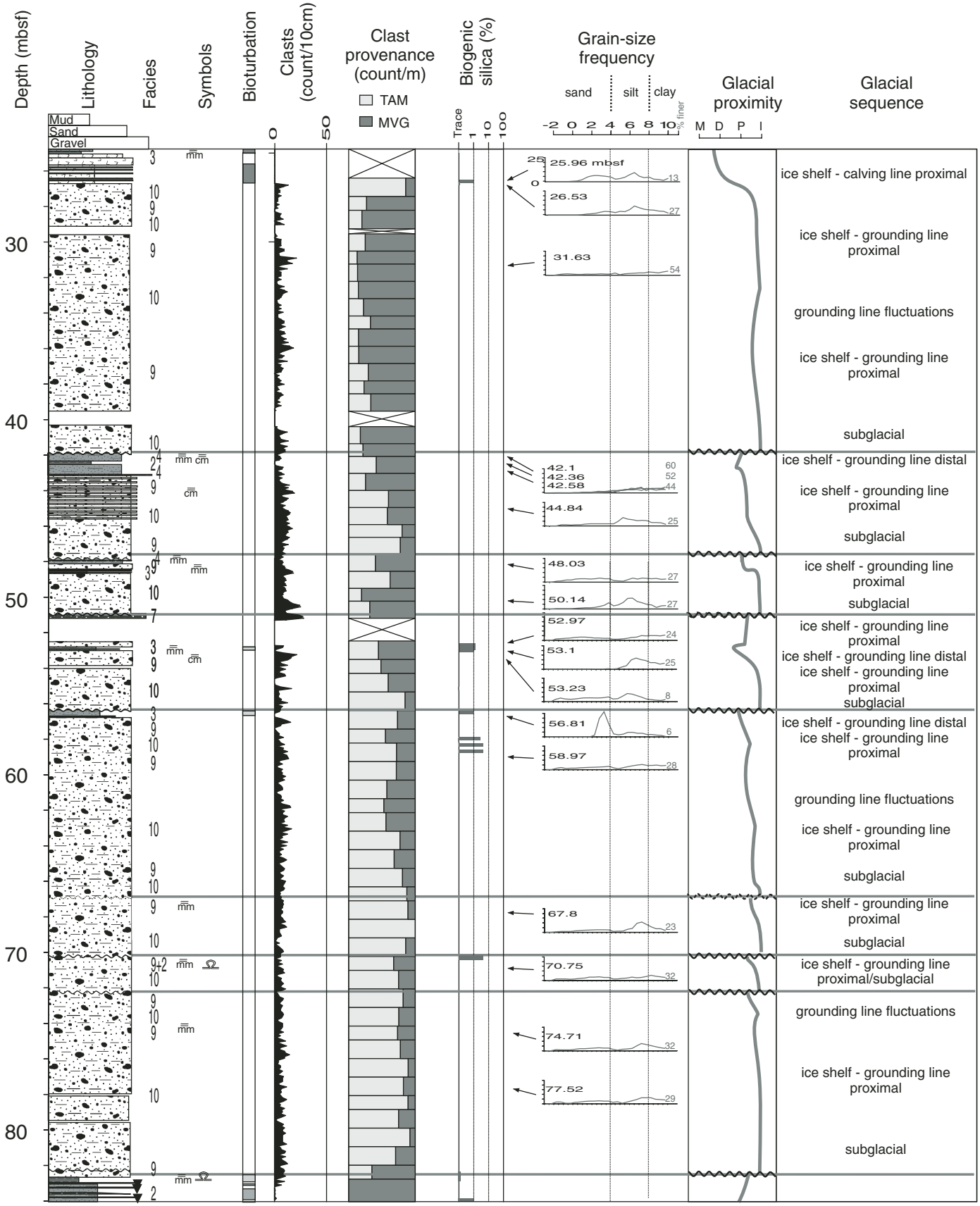

Figure 3.

Figure 3. Example stratigraphic log of motif 1 sequences from AND-1B (25–84 m below seafloor [mbsf]). Interpretations are based on the facies deposition model. Facies numbers are given in Table 2. Key to symbols, bioturbation, glacial proximity, and lithologies is provided in Figure 2. TAM—Transantarctic Mountains; MVG—McMurdo Volcanic Group.

that is similar to subglacial tills cored in the central Ross Sea (Anderson et al., 1980; Mosola and Anderson, 2006). In addition, the location of diamictites interpreted as tills is consistent within the sequence architecture that we define in this paper, where there is a logical vertical succession of facies documenting the transition of grounded ice into a glacimarine depositional environment. As discussed earlier, subglacial and ice-proximal deposition in AND-1B, where identified by the previous criteria, is interpreted as being deposited beneath a laterally extensive marine-based ice sheet across the Ross Embayment, where a terminus may have extended well beyond the drill site out into the Ross Sea.

Mass-flow deposits are common facies from Holocene cores collected within McMurdo Sound itself (e.g., Bartek and Anderson, 1992; Carter et al., 2007; McKay et al., 2008). Coarse-grained (sands and gravels) facies within these mass-flow deposits are thin (<1 m) and interstratified with mudstones; contain biogenic silica; have a predominance of volcanic clasts; have a more varied matrix texture with distinct modes; may contain evidence of bioturbation at the top of the unit; and have sharp basal contacts with rip-up clasts incorporated into the overlying unit (Carter et al., 2007; McKay et al., 2008). In addition, the volcanic evolution of the basin suggests that volcanic debris flows are less likely below 150 mbsf (meters below seafloor), due to the absence of the Hut Point Peninsula (and a smaller Ross Island) prior to this time (ca. 1.3 Ma; Esser et al., 2004), which would result in a reduced depositional slope. Holocene cores from beneath the McMurdo Ice Shelf and in the Lewis Basin to the north of Ross Island show less evidence of mass flows (McKay et al., 2008). These sequences are also stratigraphically consistent with subglacial to open-marine sequences in the Ross Sea (Domack et al., 1999). In AND-1B, mass flows are distinguished from tills or glacimarine deposits on the basis of sharp, undulating basal contacts, the presence of rip-up clasts derived from immediately underlying facies, a dominant volcanic clast content, or evidence of rotational structures such as accretionary "halos" of matrix surrounding clasts. Mass flows deposited due to proglacial processes at the ice-sheet grounding line are more difficult to discriminate, but this distinction is less critical for our interpretations since they represent a grounded ice sheet in the immediate vicinity of the drill site.

Glacimarine and Open-Marine Facies

Several facies commonly associated with proximal glacimarine deposition are noted in AND-1B (Table 2), including mudstone with dispersed clasts, conglomerates, sorted sandstone (with a Transantarctic Mountains provenance), conglomerates, and rhythmically interlaminated couplets of claystone with either siltstone or very fine-grained sandstone (Fig. 9). These facies are described in more detail in the appendices, but the changing abundance of each throughout the core (Table 2) and comparison to modern-day analogs (Table 1) provide insight into the past extent of subglacial meltwater process. For example, the rhythmically interlaminated claystone and silt/sandstone facies in AND-1B are consistent with cyclopsam and cyclopel facies described from modern temperate to subpolar glacimarine environments in Alaska and the Greenland margin (Table 1), where they are deposited in quiet-water basins by suspension settling from meltwater plumes (Mackiewicz et al., 1984; Cowan et al., 1999; Ó Cofaigh and Dowdeswell, 2001). The rhythmicity likely resulted from turbid meltwater plumes interacting with tidal currents near the top of the water column that modulated the settling of suspended sediment to the seafloor (Cowan et al., 1999). Laminate couplets of this type (i.e., cyclopsams and cyclopels) and thickness are not documented in modern-day Antarctic glacimarine settings, yet they are common in temperate to subpolar settings (Table 1; see appendices for detailed description).

Inclined beds of sorted and graded sandstone beds interbedded with mudstone having a Transantarctic Mountains grain provenance are indicative of proglacial fan deposits, while deposits of clast-supported conglomerates with a similar provenance that overlie subglacial tills and glacimarine diamictites provide evidence of channelized flow (i.e., subglacial conduit discharge) or grounding line fan development at the grounding line of a marine terminating ice sheet (see appendices for more detail).

During interglacials, the drill site was covered by either an ice shelf (similar to present day Ross Ice Shelf), or it was in seasonally open water when the ice sheet retreated past the AND-1B drill site, during which local deposition of marine diatoms and terrigenous mud occurred along with occasional debris from floating ice.

Chronology

The chronology used in this paper (Fig. 2) is based on the AND-1B age model published by Wilson et al. (2007). The model integrates $^{40}Ar/^{39}Ar$ ages, microfossil biostratigraphic datums, and magnetostratigraphy. The $^{40}Ar/^{39}Ar$ dating of 14 volcanic samples from six stratigraphic horizons in AND-1B provides the primary numeric age control (Wilson et al., 2007; Naish, 2009; Fig. 2). Pliocene-Pleistocene diatom floras are abundant within the upper 600 m of AND-1B, and a high-resolution diatom biostratigraphy has been developed for this interval (Wilson et al., 2007; Naish et al., 2009). These $^{40}Ar/^{39}Ar$ and biostratigraphic data provide excellent correlation of the magnetic polarity stratigraphy to the geomagnetic polarity time scale of the Pliocene-Pleistocene interval of the AND-1B core (Wilson et al., 2007; Naish et al., 2009). This integrated chronology identifies several unconformities in the upper 600 m of the core that have likely resulted from nondeposition and/or erosion through long-term tectonic influences and shorter-term glacial processes. However, the rate of basin subsidence has been high enough to provide sufficient accommodation space to allow for intervals of relatively continuous deposition. During the Pliocene-Pleistocene, five relatively continuous stratigraphic windows are identified in the upper 600 m: (1) the early Pliocene between 600 and 460 mbsf (ca. 4.9–4.6 Ma); (2) the mid-Pliocene between 440 and 280 mbsf (ca. 3.6–3.2 Ma); (3) the Late Pliocene between 253 and 150 mbsf (ca. 2.75–2.35 Ma); (4) the early Pleistocene between 150 and 80 mbsf (a relatively discontinuous record between ca. 1.7 and 1 Ma); and (5) the late Pleistocene between 80 and 20 mbsf (ca. 0.78–0.1 Ma).

A thick interval of near-pure volcaniclastic sandstone, mudstones, and breccias dominates the core between ~759 and ~586 mbsf, and a basaltic lava flow at 648.37 mbsf is $^{40}Ar/^{39}Ar$ dated at 6.48 (±0.13) Ma (Wilson et al., 2007). The continuous volcanic nature of this interval suggests that it is a single eruptive sequence with a much higher sedimentation rate than the rest of the sequences in AND-1B.

At present, due to a relative lack of diatoms and primary volcanic ashes, the chronology

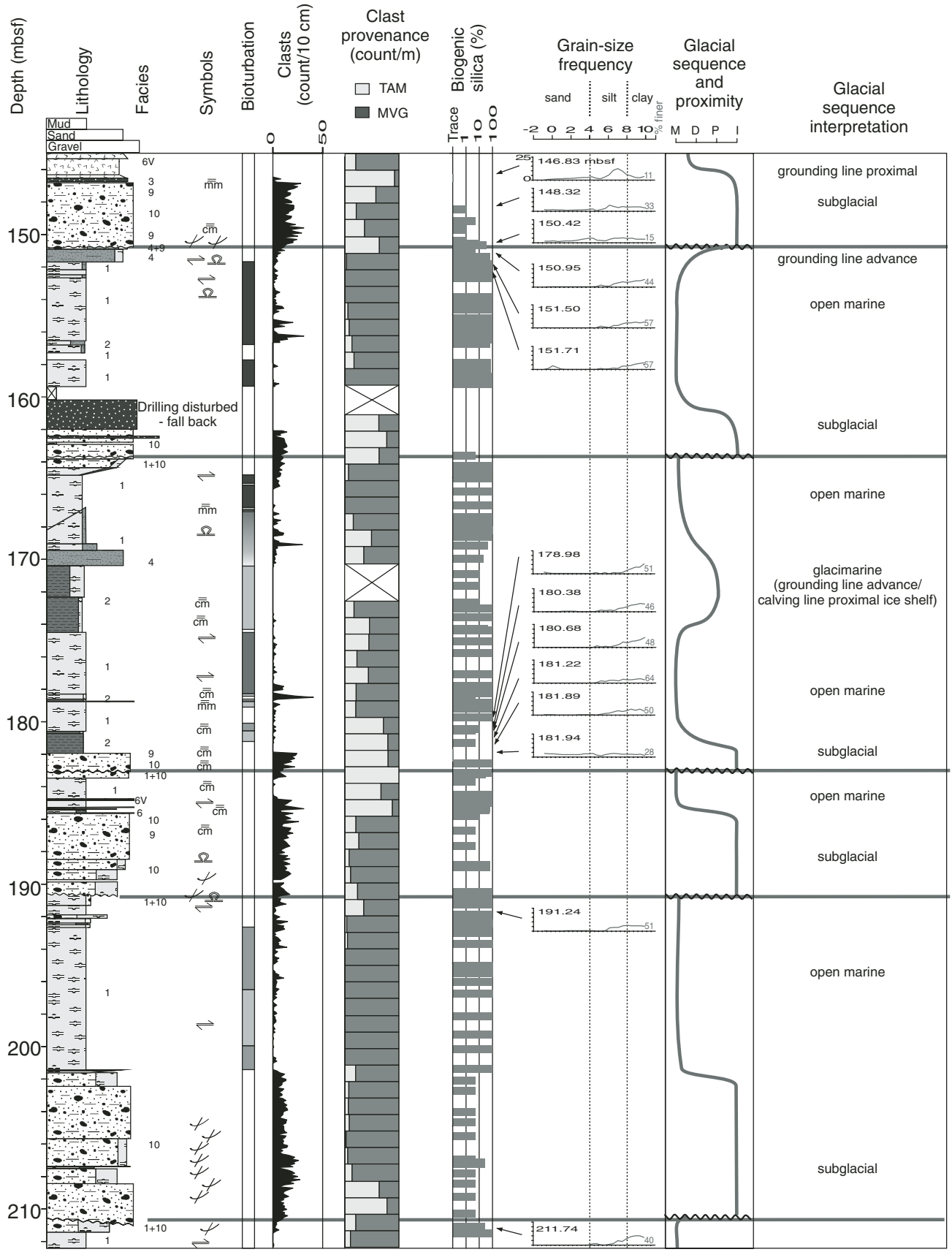

Figure 4.

Figure 4. Example stratigraphic log of motif 2a sequences from AND-1B (145–212 mbsf). Interpretations are based on the facies deposition model. Facies numbers are given in Table 2. Key to symbols, bioturbation, glacial proximity, and lithologies is provided in Figure 2. TAM—Transantarctic Mountains; MVG—McMurdo Volcanic Group.

below 759 mbsf is constrained only by the date of the basaltic lava flow at 648.37 mbsf and $^{40}Ar/^{39}Ar$ dates from three separate volcanic clasts within a volcanic glass–bearing diamictite between 1277.91 and 1279.04 mbsf (Wilson et al., 2007). These clasts yielded ages of 13.82 ± 0.09 Ma, 13.85 ± 0.18 Ma, and 13.57 ± 0.13 Ma, and they provide a maximum depositional age of 13.57 ± 0.13 Ma. The tight grouping of these ages suggests that this was the likely depositional age for this deposit, indicating that the Middle to Late Miocene is represented between 1285 and 759 mbsf in AND-1B, although comparisons to the Pliocene interval suggest there are probably numerous unconformities in this interval.

SEQUENCE STRATIGRAPHIC FRAMEWORK

We recognize 58 unconformity-bounded glacimarine sequences in the AND-1B core (Fig. 2). Each sequence base is placed at an unconformity interpreted as a glacial surface of erosion (after Fielding et al., 2000), which are identified on the basis of sharp facies dislocations separating massive diamictite from underlying facies that are usually deformed and/or intermixed (e.g., Fig. 7B), as discussed earlier.

Each glacial surface of erosion is overlain by a vertical succession of lithofacies that we interpret as recording: (1) the retreat of grounded ice from the site, after a glacial advance and maximum; and after grounding line retreat, (2) the development of ice-shelf, and then perhaps open-marine, conditions during a glacial minimum. Subsequent ice readvance led to glacial overriding and development of the overlying glacial surface of erosion. Variations in lithofacies with time primarily reflect changes in depositional energy, which we interpret to reflect changes in glacial proximity. Glacial surfaces of erosion and glacimarine sequences are not evident in the volcanic successions between 759.33 and 558.75 mbsf, and between 1275 and 1220 mbsf. Although there is considerable lithological variation within these glacial-interglacial sequences, we identify three characteristic facies successions, termed motifs (Figs. 3–6), that we interpret as recording deposition under distinctly different glacial regimes. The relative abundances of lithofacies within each motif are detailed in Table 2.

Motif 1: Diamictite Dominant

The basal portion of motif 1 is a massive diamictite (facies 10, 68% of the total motif 1 facies assemblage), 3–30 m thick, that passes upward into stratified diamictite (facies 9, 24% of the total motif 1 facies assemblage). The basal diamictites are usually overlain by thin (0.2–6-m-thick) beds of mudstone with dispersed clasts (facies 4) and silty claystone (facies 2), with or without interstratified volcanic sandstone. Figure 3 shows eight examples of motif 1 between 84 and 25 mbsf in AND-1B. Sequences exhibit a sharp base underlain by deformed and often stratified diamictite (facies 9), interstratified sandstone and mudstone (facies 3), sandstone (facies 6), or mudstone (facies 2) of the underlying sequence (e.g., Fig. 7B). Sediments directly above and below the glacial surface of erosion often display evidence of soft-sediment deformation and shearing, along with clastic intrusions. In addition, the massive diamictites qualitatively display horizontal alignment of clasts, which is suggestive of shearing by glacial overriding. This, together with the criteria outlined earlier in this paper for identifying subglacial conditions, suggest deposition beneath grounded ice. These diamictite facies are interpreted to record periods of grounded ice or proximal glacimarine sedimentation at the site. Diatom-poor, finer-grained facies that lack an ice-rafted component are inferred to have been deposited in a low-energy environment beneath an ice shelf, while interbedded mudstone and sandstone facies are inferred to represent proximal glacimarine settings, such as near a grounding line or beneath an ice shelf. Motif 1 dominates the upper 82.7 m of the core (late Pleistocene) and the interval between 1285 and 1083 mbsf (late Middle Miocene), except for the volcanogenic interval between 1275 and 1168 mbsf (see Fig. 2).

Motif 2: Interstratified Diamictite and Diatomite

Sequences of motif 2 dominate the stratigraphic section between 586.59 and 82.7 mbsf (Fig. 2). Each sequence has a basal massive diamictite, >1–20 m thick (facies 10, 31% of the total motif 2 facies assemblage), deposited during a glacial maximum. The basal diamictite is overlain by a grounding line retreat succession of stratified diamictite (facies 9, 3% of the total motif 2 facies assemblage) or mudstone with dispersed clasts (facies 4). The grounding line retreat succession passes upward into increasingly more ice-distal and open-marine deposits, including glacimarine biosiliceous mudstone with iceberg-rafted debris (e.g., facies 3 and 4) and open-marine diatomite (facies 1, 37% of the total motif 2 facies assemblage) with minor or rare iceberg-rafted debris. The diatomite records the most open-water and ice-distal depositional conditions developed during the glacial minimum. The diatomite units range up to 84 m thick (e.g., 460–376 mbsf), lack significant terrigenous mud, and contain volcanic sandstone layers, interpreted as slightly reworked ash layers, that are rare but also consistent with open-water conditions. Although rare compared to other facies, the volcanic facies are abundant compared to what has been seen in other Antarctic cores and reflect local active volcanism that is preserved during interglacials. Facies that record glacial readvance may be present above the diatomite in motif 2, and they consist of mudstone- and sandstone-rich facies (facies 2, 3, and 4). This record of glacial readvance is overlain by stratified diamictites immediately below the next glacial surface of erosion

We have subdivided motif 2 into two "submotifs" distinguished by the extent of terrigenous sedimentation during the glacial minimum and retreat/advance phases. Motif 2a (316.2–150.7 mbsf) contains diatomite with a minor (<10%) terrigenous component throughout, and retreat and advance successions are generally 1–2 m thick (e.g., Fig. 4). The glacial minimum in motif 2b (150.7–82.7 mbsf; 586–316.2 mbsf) is recorded by terrigenous-bearing to terrigenous-rich diatomites (i.e., containing 10%–50% terrigenous material), and thicker retreat and advance successions of mudstone-rich facies (e.g., Fig. 5). Soft-sediment deformation features, clastic dikes, fractures, and brecciation immediately below the glacial surface of erosions in motif 2 are attributed to subglacial deformation and/or ice pushing near the grounding line during glacial advance. Above 316.2 mbsf, the readvance successions often are truncated by a glacial surface of erosion overlain by a thick massive diamictite. The diatomite below the glacial surface of erosion typically is deformed, sheared, and intermixed with the subglacial till that lies above that glacial surface of erosion (e.g., Fig. 8A).

Motif 3: Interstratifed Diamictite and Mudstone

Motif 3 dominates the interval between 1083 and 770 mbsf in AND-1B and displays some similarities to motif 2, but it lacks diatomite

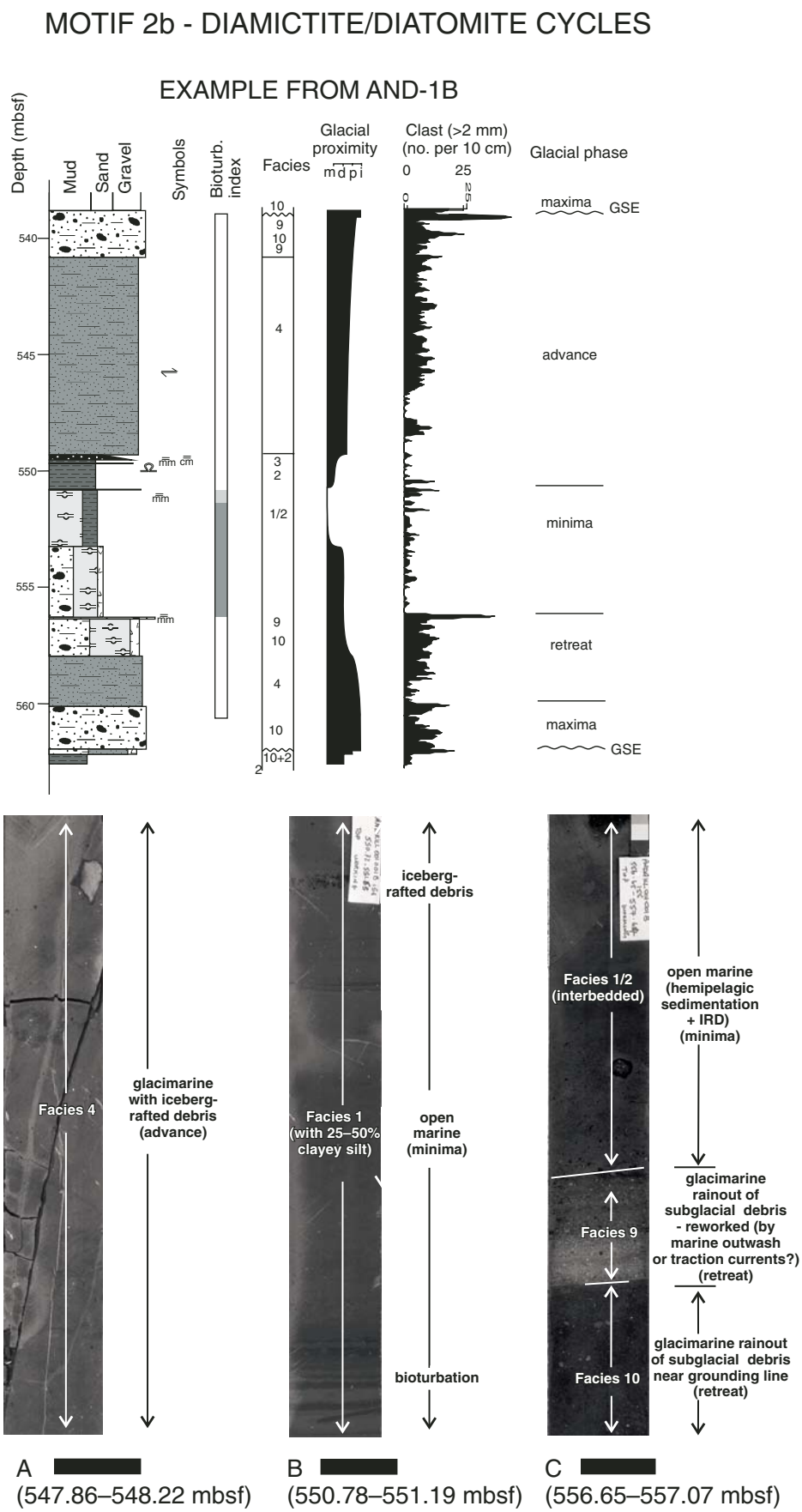

Figure 5. Example stratigraphic log of a motif 2b sequence from AND-1B (539.00–563.80 mbsf) and representative photos of facies assemblages within motif 2b. Interpretations are based on the facies deposition model. Facies numbers are given in Table 2. Key to symbols, bioturbation, glacial proximity, and lithologies is provided in Figure 2. GSE—glacial surface of erosion; IRD—iceberg-rafted debris. TAM—Transantarctic Mountains; MVG—McMurdo Volcanic Group. Black scale bar is 5 cm.

and is composed almost entirely of diamictite (facies 9, 10; 29% of the total motif 3 facies assemblage) and terrigenous mudstone-rich facies (facies 2, 3, 4, and 5; 67% of the facies assemblage within motif 3) (e.g., Fig. 6). The facies assemblages associated with grounding line retreat and readvance (e.g., facies 3–5) generally are 10–40 m thick in motif 3 (e.g., Figs. 2 and 6), which is thicker than their equivalents in motif 2. This thickness difference may imply a higher sedimentation rate for motif 3 than for motif 2. In all cases of motif 3, a thin massive diamictite (facies 10) overlies the glacial surface of erosion, and this is interpreted as tillite deposited during a glacial maximum. This massive diamictite is overlain by interstratified diamictite (facies 9 and 10), which pass upward into interbeds of rhythmically interlaminated mudstone and sandstone (facies 5), interstratified mudstone and sandstone (facies 3), and/or mudstone (facies 2). Conglomerate (facies 7) and mudstone with dispersed clasts (facies 4) also are common within this sequence. Between 1083 and 900 mbsf, there are nine well-defined motif 3 sequences, each of which shows a transition from massive diamictite with Transantarctic Mountains–derived clasts passing up into a succession of glacimarine facies, including stratified diamictite, sandstone, cyclopels/cyclopsams, and mudstone (e.g., Fig. 6). Between ~900 and 780 mbsf, subglacial deposition and glacial surfaces of erosion are difficult to

Figure 6. Example stratigraphic log of motif 3 sequences from AND-1B (1000–1066.00 mbsf). Interpretations are based on the facies deposition model. Facies numbers are given in Table 2. Key to symbols, bioturbation, glacial proximity, and lithologies is provided in Figure 2. TAM—Transantarctic Mountains; MVG—McMurdo Volcanic Group.

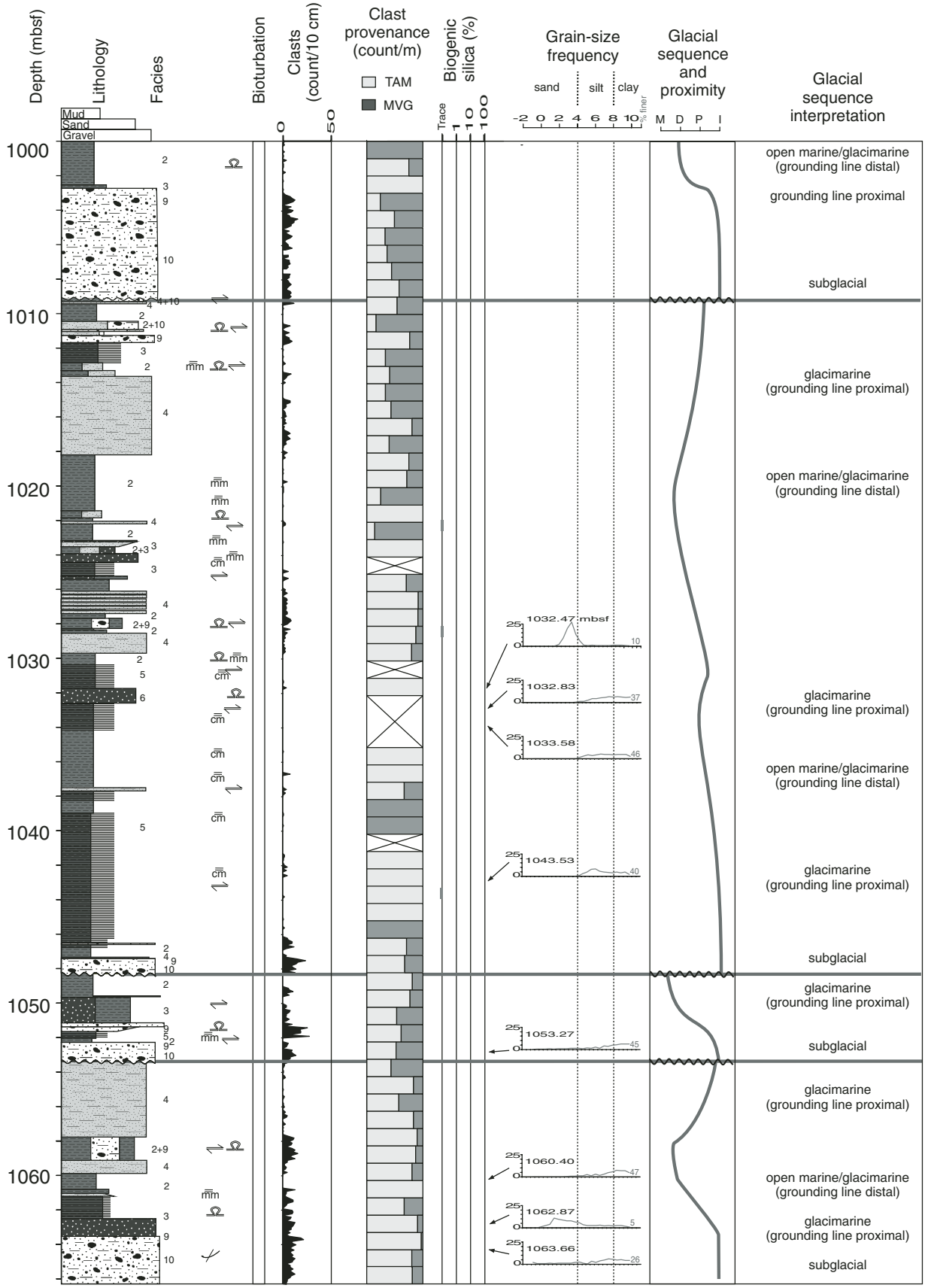

Figure 6.

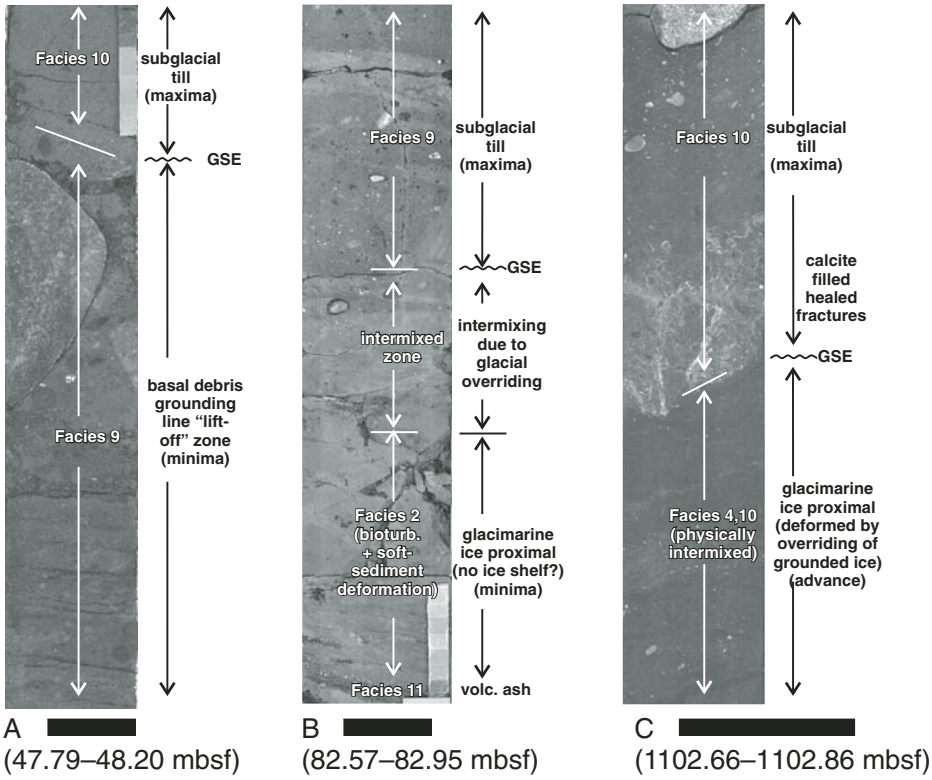

Figure 7. Representative photos of facies assemblages within motif 1. GSE—glacial surface of erosion. Black scale bar is 5 cm.

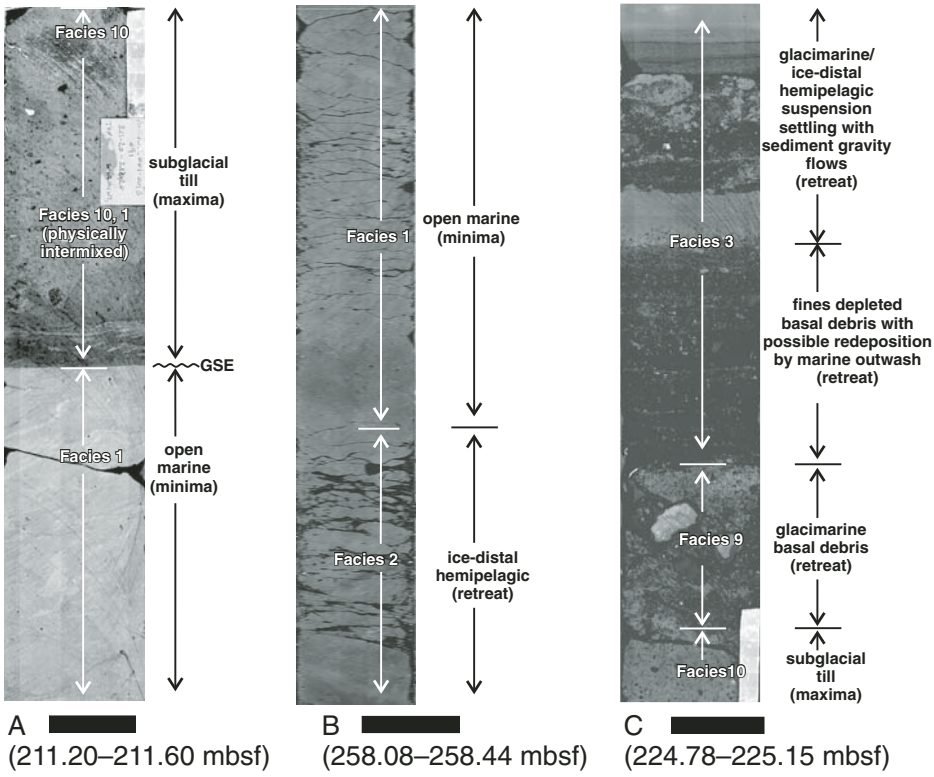

Figure 8. Representative photos of facies assemblages within motif 2a. GSE—glacial surface of erosion. Black scale bar is 5 cm.

identify because a pervasive pyrite cement overprints and obscures sedimentary structures, and glacimarine facies successions are not as well-defined. As a result, we are more tentative about our identification of glacial surfaces of erosion and sequences between 900 and 780 mbsf (Fig. 2).

DISCUSSION: SEDIMENTATION MODELS OF GLACIMARINE DEPOSITION AT AND-1B

Sedimentation during a Cold, Polar Glacial Regime

Motif 1 is consistent with sedimentary models previously derived from the study of modern processes and glacial systems in cold polar regimes, and from successions deposited during the retreat of the Antarctic Ice Sheet in the Ross Embayment since the Last Glacial Maximum. However, motif 1 notably lacks open-marine diatom-bearing/rich mudstone and diatomite, similar to those forming in the present-day Ross Sea (e.g., Domack et al., 1999; Dunbar et al., 1989; McKay et al., 2008; Sjunneskog and Scherer, 2005), and there is also a near-complete absence of reworked diatoms within the diamictite facies. The massive diamictites generally are interpreted as either subglacial till (based on the criteria outlined earlier in this paper) or proximal glacimarine deposits. Diamictites with these attributes are characteristic of Last Glacial Maximum deposits collected from the Ross Sea region (e.g., Domack et al., 1999; Licht et al., 1999). The thin interbedded sandstones and mudstones, as well as diamictites with well-defined stratification, are similar to modern sediments collected from the sub–ice-shelf zone beneath the McMurdo Ice Shelf (McKay et al., 2008). Although these mudstones and sandstones are thin in motif 1 sequences, they indicate that glacial retreat and glacial minima conditions produced an ice shelf over the site during the deposition of motif 1, much like conditions at present. Open-water conditions with biogenic-dominated sedimentation are not recorded at the AND-1B drill site during deposition of motif 1 sequences.

Beneath the modern McMurdo Ice Shelf, ~60 cm of sediment has accumulated since ice-shelf conditions were initiated ca. 10,000 ^{14}C yr B.P. (McKay et al., 2008). This sedimentation rate (0.06 mm/a) is much lower than the rate for open-water diatomaceous ooze (~0.2 mm/a) deposited in the Ross Sea (Domack et al., 1999; McKay et al., 2008). Diatom remains are present only in trace amounts in the upper 82.7 m of AND-1B (Fig. 2; Scherer et al., 2007), despite the presence of sparsely fossiliferous mudstone and sandstone facies interpreted as sub–ice-shelf

deposits. The low diatom abundances within the diamictite facies suggest a minimal amount of erosion within this interval, because erosion of open-marine diatomite should have recycled more diatomaceous material into the overlying diamictites, as is observed in diamictites of motif 2 (Fig. 4) and of the Last Glacial Maximum from the Ross Sea (e.g., Scherer et al., 2004; Sjunneskog and Scherer, 2005). If erosion by overriding ice was so significant that all traces of underlying diatomite were removed, then it is unlikely that thin sub–ice-shelf deposits would have been preserved.

The presence of motif 1 from 1.10 Ma (Fig. 2) implies that, for several glacial-interglacial cycles, ancestral configurations of the ice sheet in the Ross Embayment were similar to the configurations of the Last Glacial Maximum to the Holocene deglaciation. Compared to its extent during the Pliocene, an expanded ice sheet or ice shelf persisted in the Ross Embayment for extended periods, as recorded by the Middle to Upper Pleistocene and Middle Miocene sections of AND-1B, even in a relatively deep-water setting. We infer that the glacial regime during deposition of motif 1 was similar to the regime of the last glacial cycle—an ice sheet that had a cold polar glacial regime, i.e., a vertical temperature profile entirely below freezing with negligible surface melting and subglacial outwash. Ablation of this ice sheet was likely controlled by sub–ice-shelf melting and calving at the ice-shelf margins, so oceanic temperature and circulation, and eustatic sea-level change were the major controls on ice-volume fluctuations. In the Ross Sea, this regime persisted through the mid- to late Pleistocene and in Middle to early Late Miocene time. A cold polar regime during the Middle to early Late Miocene is consistent with a previous interpretation made from seismic profiles indicating large-scale expansion of the ice sheet onto the Ross Sea continental shelf sometime between ca. 13 and 10 Ma (De Santis et al., 1995), and may correspond to Bart's (2003) Middle to Late Miocene grounding events (RSU3.2 and RSU3.1). In addition, the expansion of a large ice sheet in the Ross Embayment may be represented in the marine $\delta^{18}O$ record in the form of large negative excursions (termed Mi-events) that are believed to represent large-scale Antarctic glaciations during the Middle Miocene (e.g., Mi-4, Mi-5; Miller et al., 1991).

The sedimentation model for motif 1 (Fig. 10) also incorporates interpretations made from the drill cores collected closer to the Victoria Land coast (e.g., CIROS-2). This model shows the damming of the mouth of Ferrar Fjord by an expanded ice sheet in the Ross Embayment during glacial maxima, which was interpreted to have caused deposition of glaciolacustrine rhythmites in CIROS-2 (Barrett and Hambrey, 1992). Based on the interpretation that unconformities are minor within the Pleistocene section of motif 1, interglacial sedimentation at AND-1B occurred almost entirely by sub–ice-shelf processes with hemipelagic deposition and sediment gravity flows associated with grounding line retreat/advance. Where the upper parts of motif 1 contain locally derived McMurdo Volcanic Group sediments (Fig. 1), we infer a depositional environment proximal to the calving line, probably similar to present-day conditions at AND-1B.

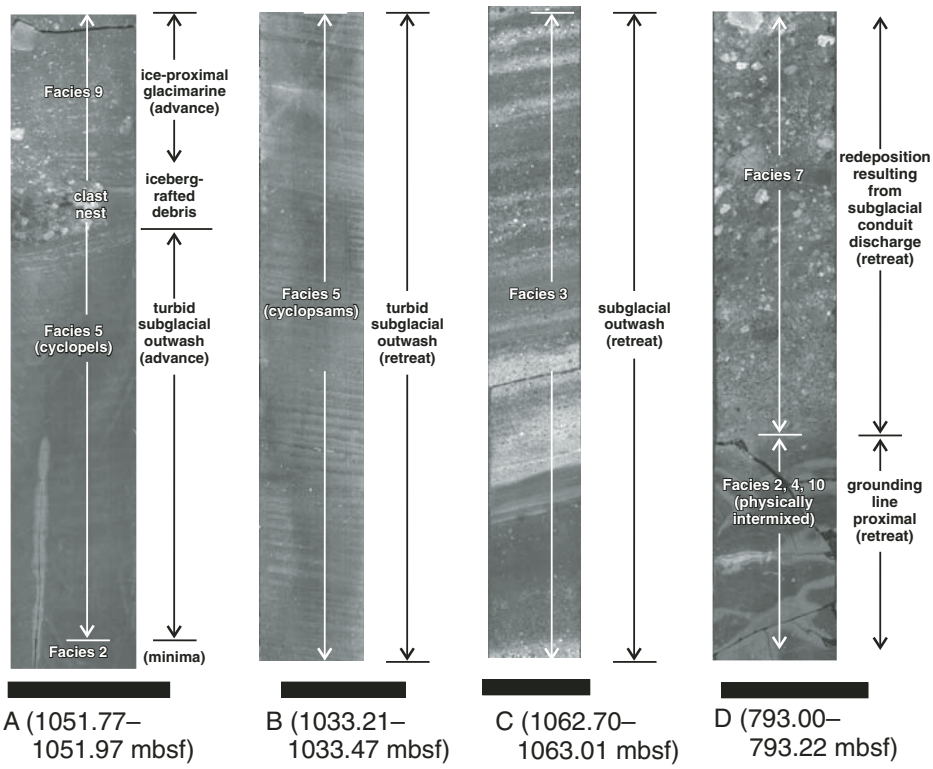

Figure 9. Representative photos of facies assemblages within motif 3. Black scale bar is 5 cm.

Sedimentation during a Dynamic Polar and/or Subpolar Glacial Regime

Motif 2 records more dynamic fluctuations of the ice sheet than motif 1. Motif 2 sequences dominate the Pliocene section of AND-1B, and they are most notable for repeated couplets of diamictite (34% of the total facies assemblage) and diatomite (37% of the total facies assemblage). The diamictites are interpreted as subglacial till deposited during glacial maxima, whereas the diatomites record open-marine settings during glacial minima. The lack of terrigenous fine-grained sediment (i.e., not iceberg-rafted debris) within or associated with the diatomites implies a lack of subglacial meltwater entering the Ross Embayment during glacial minima. Episodes with greater meltwater supply may be recorded by the muddy proglacial facies (constituting ~10%–25% of some sequences; Fig. 2) included in glacial retreat and advance sequences in motif 2b (586.59–346 mbsf).

Motif 2 records a more dynamic ice-sheet system in the Ross Embayment than the mid- to late Pleistocene, with periods of open-water deposition (see Fig. 11) during glacial minima. The 84-m-thick diatomite above 459.24 mbsf indicates open-marine conditions in the Ross Embayment for at least 0.2 Ma, and the presence of hiatus in this unit suggests open water conditions may have persisted for much longer (Naish et al., 2009).

Diatomites deposited during the Holocene have been documented from basinal settings similar to the setting of AND-1B but located immediately north of Ross Island (McKay et al., 2008) and farther north in the Ross Sea (e.g., Domack et al., 1999). These Holocene deposits indicate that diatomites can accumulate close to an ice-shelf calving line, so the Pliocene calving line did not have to retreat significantly from the present-day calving-line position to allow deposition of diatom muds and oozes at AND-1B. The development of the Hut Point Peninsula at ca. 1.3 Ma (Kyle, 1981) may have created a new pinning point for the retreating ice-shelf

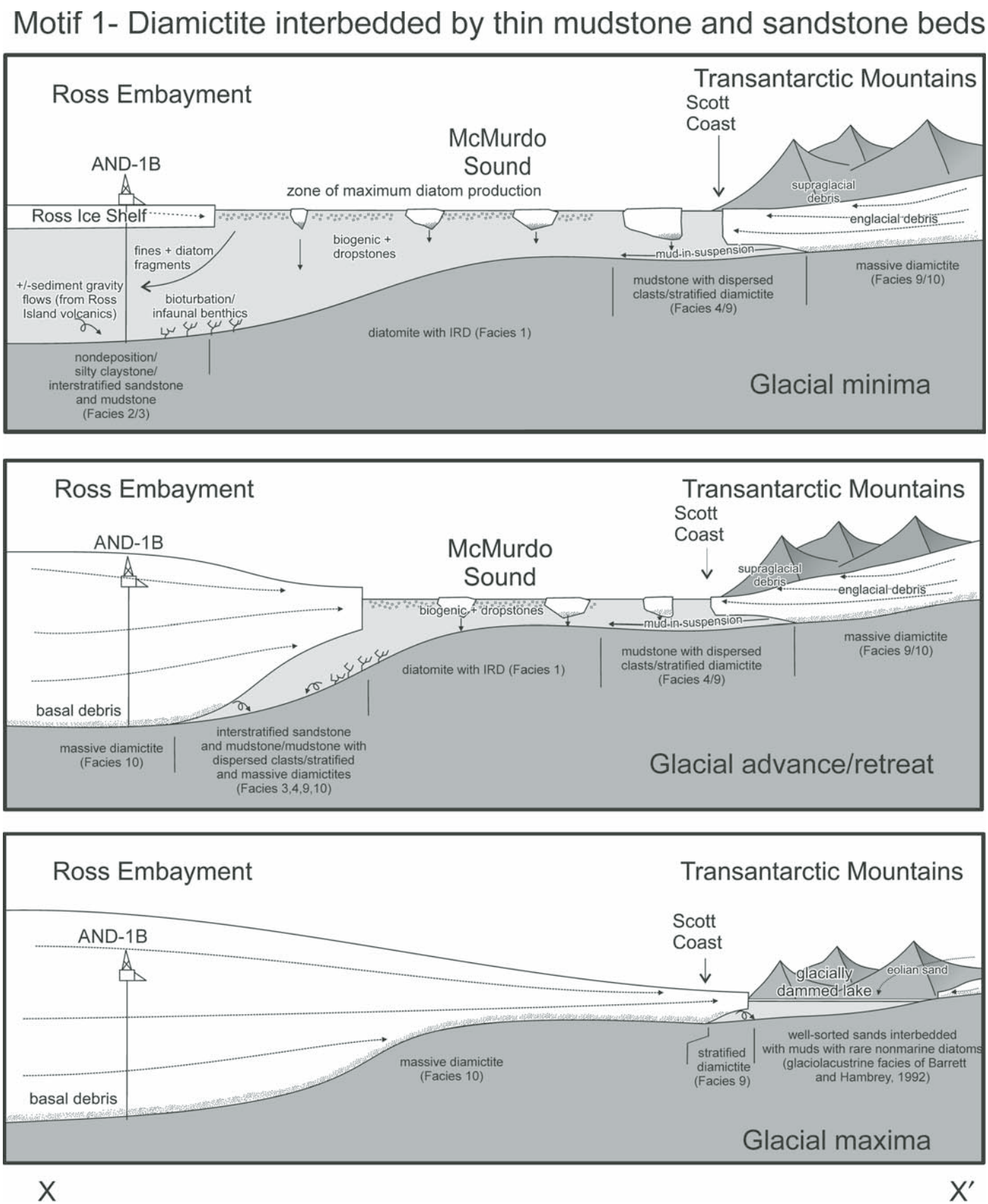

Figure 10.

Figure 10. Sedimentary model for motif 1, along a generalized profile of transect x-x′ (see Fig. 1). Glacial minima (top) at the drill site are characterized by sub–ice-shelf deposition of mudstone interbedded with sediment gravity flows of volcanogenic sandstone. Facies associated with glacial advance/retreat (middle) of ice sheet over the AND-1B drill site lack significant subglacial meltwater. During glacial maxima (bottom), grounded ice occupied McMurdo Sound (and the Ross Sea), which resulted in the formation of "ice dammed" lakes during the Pleistocene (e.g., Hall et al., 2000; Barrett and Hambrey, 1992). IRD—iceberg-rafted debris.

calving line, creating a potential complication in interpreting the paleoclimatic signal. However, several indicators of conditions warmer than present do accompany the AND-1B diatomites. While the transitions from glacial to open-marine facies are stratigraphically thinner in motif 2 than in motif 3, the transitions in motif 2b display clear evidence of elevated rates of sediment delivery (compared to motif 1 and 2a). Evidence is also present that sedimentation in motif 2b was influenced by some subglacial meltwater discharge during advance and retreat of the grounding line. This evidence includes ~5- to 10-m-thick intervals of massive mudstone (facies 2), mudstone with dispersed to common clasts (facies 4), and graded/stratified outwash sandstone interbedded with mudstone (facies 3) that contains tractional sedimentary structures, such as ripple cross-stratification, inferred to be related to meltwater discharge (Table 2; Fig. 2). These facies commonly lie directly on top of stratified and massive diamictites deposited by grounded ice and during ice lift-off. Preliminary analysis of diatom assemblages also provides strong evidence of warmer-than-present surface waters during the deposition of the Pliocene diatomites (Scherer et al., 2007; Naish et al., 2009).

Figure 11 presents a model for the deposition of motif 2 sequences. During retreat of grounded ice, sedimentation at AND-1B was influenced by variable amounts of meltwater (motif 2a versus 2b) from the ice-sheet grounding line. Deposition during glacial minima occurred in open-water conditions, with little or no terrigenous input from East Antarctic Ice Sheet outlet glaciers or the ice sheet in the Ross Embayment via glacimarine or coastal processes. Although motif 2 is interpreted to record a more dynamic ice sheet in the Ross Embayment, it may also reflect moderate warming relative to present-day conditions. Under warmer conditions, large ice shelves were not sustained during glacial minima in the Ross Embayment, so that the glacial minima are represented by open-water sediments, rather than those deposited beneath an ice shelf.

In some cases, the transition from massive diamictite deposited beneath grounded ice to marine diatomite with a negligible terrigenous component occurs within 1 m (e.g., 225.20–224.20 mbsf), suggesting minimal meltwater associated with ice retreat and transition from a grounded ice sheet to an ice-free Ross Embayment. These thin intervals of transitional facies are most common in motif 2a between 346–150.7 mbsf (Upper Pliocene). The upsection increase in top-truncation of the sequences in the Upper Pliocene may indicate greater erosion during glacial readvance (either due to larger ice volume or a decrease in basin subsidence), or it may reflect original deposition of thin readvance successions (i.e., limited meltwater discharge).

We interpret motif 2 to reflect an increased degree of dynamism of the ice sheet in the Ross Embayment under a subpolar to polar glacial regime that was warmer than present but cooler than conditions during the deposition of motif 3. If the ice sheet had largely withdrawn from the Ross Embayment during the glacial minima recorded in motif 2, then the lack of terrigenous sedimentation at AND-1B during those minima indicates limited sediment delivery from local East Antarctic Ice Sheet outlet glaciers. This suggests that glacial regimes along the margin of the East Antarctic Ice Sheet and for the Transantarctic Mountains outlet glaciers were polar and included little to no meltwater production. However, motif 2b sequences record a warmer ice sheet in the Ross Embayment and episodic meltwater production that delivered moderate volumes of terrigenous sediment to the grounding zone during times of glacial retreat and advance. Local glaciation in the Transantarctic Mountains was similar to conditions in modern subpolar to polar environments dominated by iceberg production (see Table 1) during the deposition of motif 2a sequences in the Late Pliocene. Similar conditions, but with an increased meltwater influence, are interpreted to have existed during the deposition of motif 2b in the early Pliocene (Fig. 2). The increased abundance of terrigenous mudstone facies in motif 2 sequences between 150.70 and 82.7 mbsf, within glacial minima, retreat, and advance sequences (Fig. 2), is associated with the presence of volcanic sandstone turbidites and debris-flow deposits. Rather than representing a significant paleoclimatic change, this increased mud input probably records increased slope instability during volcanic cone building on Ross Island, especially on Hut Point Peninsula.

It is apparent from the subglacially deposited diamictites in motif 2 that despite warmer-than-present temperatures and glacial regimes during the Pliocene, expansion of the ice sheet onto the Ross Sea continental shelf still occurred. This confirms interpretations from Ross Sea seismic stratigraphy of grounding line fluctuations across the continental shelf throughout the Pliocene (Alonso et al., 1992; Bart et al., 2000; Bart, 2001). However, the record in AND-1B indicates this was a higher-frequency event—35 unconformity-bound cycles are preserved in the Pliocene-Pleistocene interval of AND-1B (Fig. 2) compared to the eight Pliocene-Pleistocene seismic units of Bart et al. (2000).

Our interpretation of the AND-1B record is consistent with Neogene strata from the Prydz Bay region of East Antarctica. The Pliocene-age Bardin Bluff deposits in the Pagodroma Group indicate that glaciers in the Lambert Fjord terminated as tidewater cliffs, rather than an ice shelf, as is the case for the present interglacial (Hambrey and McKelvey, 2000). The presence of early Pliocene marine deposits at Marine Plain in the Vestfold Hills indicates that there was some recession of the marine-based margin of East Antarctic Ice Sheet during glacial minima in Pliocene times (Quilty et al., 2000). These observations are consistent with the Pliocene record in AND-1B drill core, where periods of open-water conditions in the Ross Embayment dominate during interglacials, and ice shelves were not sustained throughout glacial minima (e.g., motif 2). The evidence from AND-1B and the on-land Prydz Bay record suggest that the marine-based sectors of the West Antarctic Ice Sheet and East Antarctic Ice Sheet both had warmer temperature profiles (subpolar to polar) relative to the present-day cold polar environment, at least to the extent that they did not support prolonged ice-shelf conditions in these large embayments during glacial minima.

Sedimentation during a Dynamic Subpolar Glacial Regime

Motif 3 is interpreted as the record of glacial retreat, minimum, and advance phases dominated by deposition of terrigenous siliciclastic sediments. At the AND-1B drill site, large volumes of glacial outwash mud, supplied from nearby sources, prevented diatomite from accumulating. This mud supply suggests that significant subglacial meltwater was provided from local East Antarctic Ice Sheet outlet glaciers and the ice sheet in the Ross Embayment during

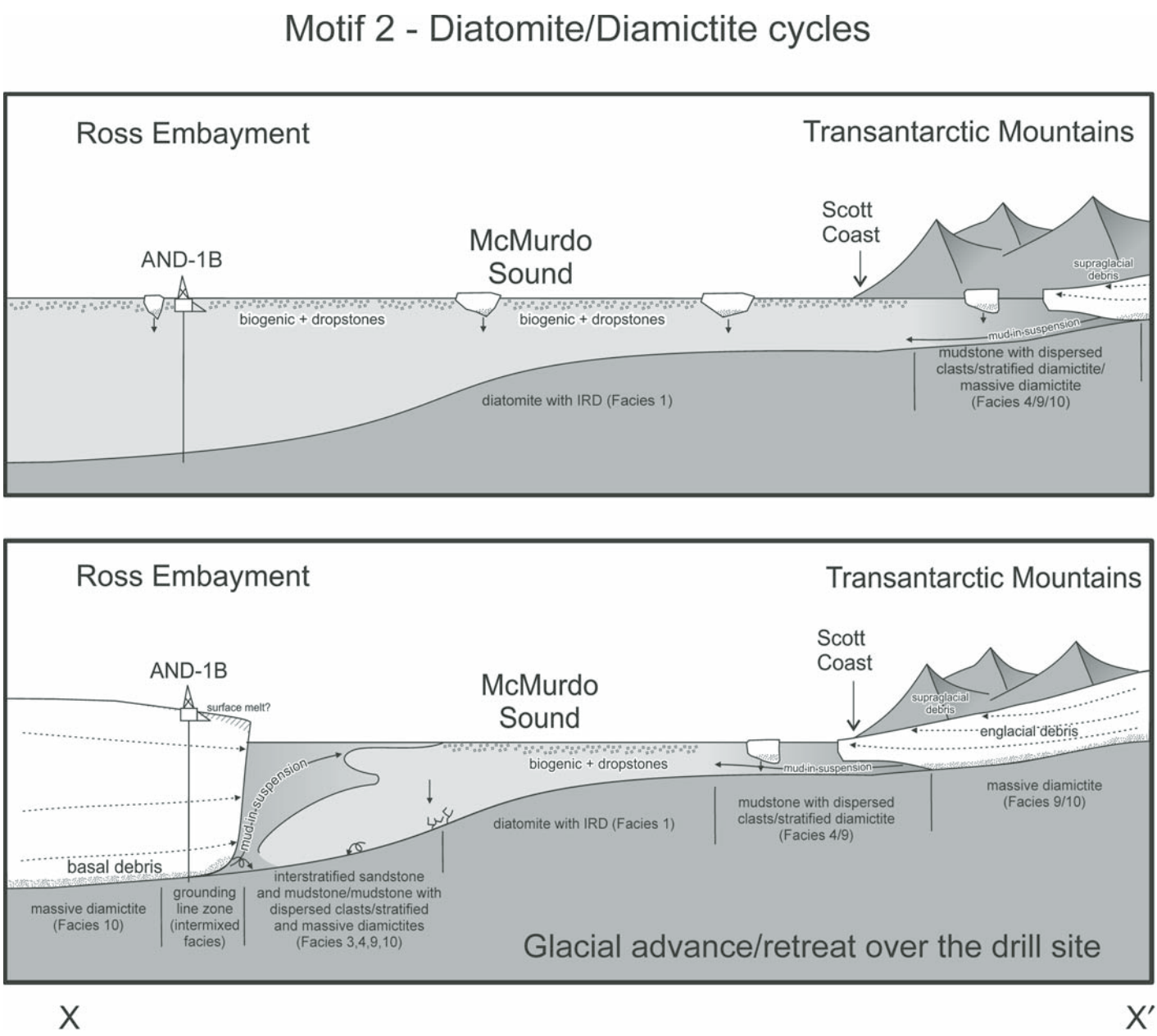

Figure 11. Sedimentary model for motif 2, along a generalized profile of transect x-x′ (see Fig. 1). During glacial minima (top), open-marine conditions prevail at the drill site with deposition of diatomaceous ooze. During ice-sheet glacial advance/retreat (bottom), processes may be similar to those in motif 1, although sequences within motif 2b display evidence of an increased meltwater process at the grounding line. During glacial maxima, conditions were likely similar to that for motif 1 (Fig. 10), although CIROS-2 sediments are dominated by subglacial deposition beneath an expanded Ferrar Glacier, rather than glaciolacustrine sediments (Barrett and Hambrey, 1992). IRD—iceberg-rafted debris.

glacial retreat and advance. Supporting evidence includes the greater abundance of mud-rich proglacial facies (facies 2, 3, 4, 5), which form 67% of the total facies assemblage in motif 3. Within glacial retreat and advance sequences, conglomerate (facies 7), sandstone (facies 6) with ripple cross-stratification, and rhythmically interlaminated mudstone with siltstone or sandstone (facies 5) all are more abundant than in the other two motifs. These facies likely represent deposition influenced by considerable subglacial marine outwash and mass flows near the grounding line of an expanded ice sheet in the Ross Embayment. Rhythmically interlaminated mudstone and sandstone constitute 6% of the total facies assemblage in motif 3 (whereas they are rare to absent in motifs 1 and 2), and they form intervals up to 8 m thick, with cyclopsams (sandstone-mudstone couplets) grading upward into cyclopels (siltstone-mudstone couplets; Figs. 9A and 9B). Dropstones that deform underlying laminae, and poorly sorted sandstone beds, are also associated with occurrences of facies 5. Although diatoms may have been deposited with

these muds, and subsequently destroyed by diagenesis, there is no evidence of the extremely high-productivity conditions recorded by motif 2. The dominance of siliciclastic lithofacies in motif 3 and the apparent lack of bioturbation and diatoms suggest an environment with high sedimentation rates, principally of fine-grained material, in a deep-water setting influenced by iceberg rafting. The rapid input of terrigenous mudstone during glacial minima is interpreted to have diminished biosiliceous productivity or diluted the input of biosiliceous debris.

The facies successions within motif 3 are consistent with Holocene sedimentation models for subpolar environments dominated by large and relatively consistent input of glacial outwash (cf. Table 1). These environments are dominated by suspension settling from turbid meltwater plumes, sediment gravity flows, and associated iceberg rafting (e.g., Ó Cofaigh and Dowdeswell, 2001; Dowdeswell et al., 1998). Supporting evidence in the AND-1B core includes the higher abundance of facies deposited in proximal glacial and subglacial environments (i.e., massive/stratified diamictites, conglomerates, rhythmically interlaminated mudstones, and sandstones), which are interpreted to record retreat and advance of a grounded ice sheet in the area of the drill site. Evidence for increased subglacially derived meltwater include clast-supported conglomerates with a high Transantarctic Mountains clast content (e.g., Fig. 9D) interpreted to have been deposited during turbulent discharge from subglacial conduits. Also, many sandstones are compositionally similar to underlying diamictites (Fig. 6) and contain planar and ripple laminae (e.g., Fig. 9C), suggesting the deposition within a proglacial grounding line fan system. Intervals of rhythmically interlaminated mudstone with siltstone/sandstone (facies 5) are interpreted to have been deposited during grounding line retreat in the presence of large volumes of subglacial meltwater. Cyclopsams grade upward into cyclopels, indicating the transition from a proximal to a more distal glacimarine environment. Taken together, these changes in depositional environment imply significant glacial dynamism in the Ross Embayment during the deposition of motif 3. While some of these facies (graded sands and gravels, and muds) occur in present-day West Antarctica (e.g., Pine Island Bay; Lowe and Anderson, 2002), they are rare, less well-defined, and, where present, an order of magnitude thinner (e.g., 0.5–4.5 m thick) than the outwash facies that are persistently present throughout motif 3 sequences in AND-1B (10–43 m thick; Fig. 6).

Terrigenous sediments dominate the record of deposition during the glacial minimum in motif 3, from which we infer the largest extent of subglacial melting and outwash recorded in AND-1B. This evidence of significant subglacial melting and outwash suggests major fluctuations in the volume of the marine-based ice sheet in the Ross Embayment. The deposition of mudstones during glacial minima (when the marine-based ice sheet was no longer influencing sedimentation at AND-1B) raises questions about the thermal state of the East Antarctic Ice Sheet outlet glaciers terminating into the Ross Sea during these times. In the absence of a proximal Ross Embayment ice-sheet grounding line, the persistent supply of terrigenous muds during glacial minima would require a local meltwater source. Therefore, we infer that nearby terrestrial and/or marine-terminating Transantarctic Mountains outlet glaciers provided this source, and that meltwater processes were occurring probably at the bases of the main Transantarctic Mountains outlet glaciers at this time (Fig. 12).

The evidence in AND-1B for a significantly warmer glacial regime during the Late Miocene, and increased subglacial meltwater discharge from the East Antarctic Ice Sheet margin, is supported by the on-land Fisher Bench Formation (Pagadroma Group) in Prydz Bay. Glacial retreat facies in this formation contain 2–3-m-thick intervals of rhythmically laminated clay and siltstone (consistent with our cyclopels/cyclopsams in motif 3), as well as a high proportion of boulder-cobble gravels indicative of subglacial conduit discharge (Hambrey and McKelvey, 2000). Diatom biostratigraphy suggests that the Fisher Bench Formation was deposited sometime between 12.7 and 8.5 Ma (Whitehead et al., 2004), which lies in the range of the Late Miocene motif 3 strata in AND-1B (Wilson et al., 2007).

Geomorphological studies, surface age dating, tephrochronology, and recent discoveries of moraines and fossiliferous deposits place the transition from "wet-" to "cold-based" ice at ca. 14 Ma at the edge of the East Antarctic Ice Sheet in the McMurdo region (Summerfield et al., 1999; Sugden and Denton, 2004; Marchant et al., 1996; Lewis et al., 2007). This body of work implies a persistent cold landscape at high altitudes in the Transantarctic Mountains adjacent to the Ross Embayment (and therefore AND-1B) throughout the last ~14 Ma. However, this may be consistent with the AND-1B record, as the Pliocene diatomite beds in AND-1B imply very little terrigenous sediment entering the basin despite being adjacent to (100 km to the west) a mountain range with peaks exceeding 3000 m. Although there is evidence for significant meltwater derived from Transantarctic Mountains outlet glaciers in the AND-1B record during the Late Miocene (motif 3 sequences), this may also be compatible with geomorphic evidence that "selective linear erosion" under a subpolar glacial regime formed the present-day landscape in the Dry Valleys. This requires basal melting to have occurred in the troughs of Transantarctic Mountains outlet glaciers, while at higher elevations in the Transantarctic Mountains, the ice sheet remained frozen to its bed (Sugden and Denton, 2004). Motif 3 sequences in AND-1B suggest that basal conditions of Transantarctic Mountains outlet glaciers were significantly warmer and wetter in the Late Miocene than any time since.

CONCLUSIONS

The AND-1B drill core provides the most continuous, high-resolution record of ice-sheet oscillations and evolution within the Ross Embayment over the past 13 Ma yet recovered. We have identified stratigraphic signatures for repetitive oscillations of ice-sheet extent in the Ross Embayment under three distinct glacial regimes. Under all three regimes, there is evidence of subglacial erosion and deposition by a grounded ice sheet. Ice-proximal conditions were followed by a period of proglacial-marine and/or open-marine sedimentation during retreat of the ice terminus, which was succeeded by additional proglacial-marine deposition and/or erosion during subsequent ice-sheet readvance across the Ross Embayment. Three different sedimentary sequence "motifs" record changes in ice-sheet extent and provide mass balance controls through the late Cenozoic.

During the Middle Miocene, sedimentary sequences of motif 1 were deposited beneath grounded ice and floating ice shelves. Evidence for subglacial meltwater or erosion generally is lacking in these sequences, suggesting a cold, polar glacial regime for both the West Antarctic Ice Sheet and the East Antarctic Ice Sheet during this time. Sequences deposited during the Late Miocene (motif 3) contain strong evidence for significantly higher volumes of subglacial meltwater and terrigenous sediment supply by both the marine-based ice sheet in the Ross Embayment and local East Antarctic Ice Sheet outlet glaciers. This evidence includes the repeated presence of outwash facies deposited during ice-sheet grounding-line retreat and advance, as well as the deposition of mudstone facies, rather than diatomite, during glacial minima. In contrast, the Pliocene sequences of motif 2 document dynamic fluctuations of the ice sheet across the Ross Embayment in the form of subglacial diamictites alternating with open-marine diatomites. The meltwater influence on sequences

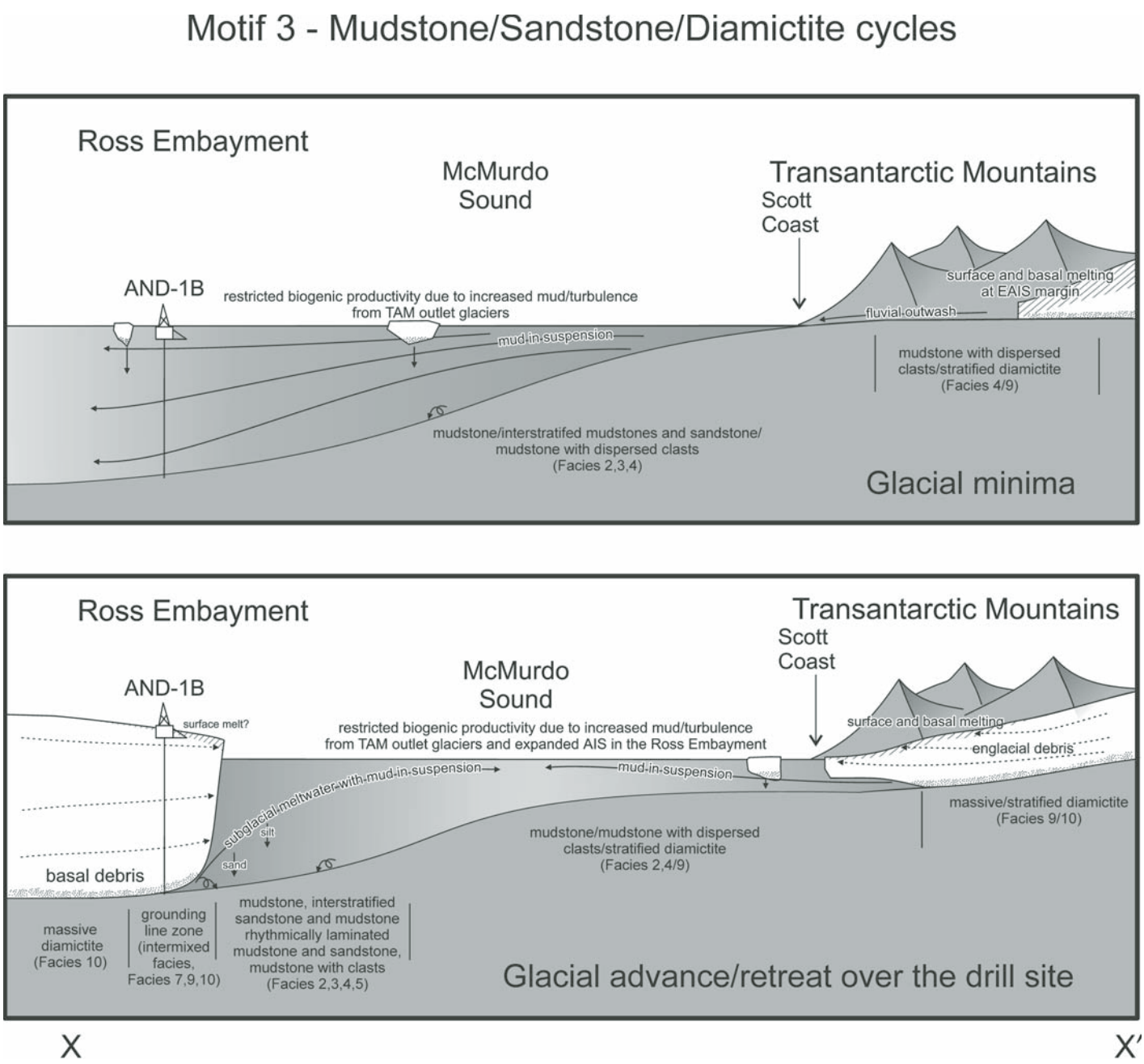

Figure 12. Sedimentary model for motif 3, along a generalized profile of transect x-x′ (see Fig. 1). During glacial minima (top), sedimentation during open-marine conditions at the drill site is dominated by hemipelagic suspension settling associated with increased meltwater derived from Transantarctic Mountains outlet glaciers, relative to motif 1 and 2. During ice-sheet glacial advance/retreat over the drill site, there is a significant increase in facies associated with meltwater process at the grounding line (facies 5, 7, 9) and other mudstone-rich facies (facies 2, 3, 4). The ice-sheet configuration for the glacial maxima is likely to be similar to that for motif 1 (Fig. 10). EAIS—East Antarctic Ice Sheet; IRD—iceberg-rafted debris; TAM—Transantarctic Mountains.

of motif 2 appears to have decreased through time, as evidenced by the progressive upsection thinning of outwash facies deposited during the transitions from subglacial to open-marine conditions. We interpret this decrease in meltwater influence as recording the transition from a subpolar glacial regime in the Early Pliocene to a polar glacial regime by the Late Pliocene. Pleistocene sequences of motif 1 record a return to full cold polar glaciations dominated by subglacial and ice-shelf deposition and a general lack of subglacial meltwater influence. This style of glaciation is consistent with present-day conditions beneath the Ross Ice Shelf.

ACKNOWLEDGMENTS

The ANDRILL project is a multinational collaboration between the Antarctic programs of Germany, Italy, New Zealand, and the United States. Antarctica New Zealand is the project operator, and it has developed the drilling system in collaboration with Alex Pyne at Victoria University of Wellington and

Webster Drilling and Enterprises Ltd. Antarctica New Zealand supported the drilling team at Scott Base, and Raytheon Polar Services supported the science team at McMurdo Station and the Crary Science and Engineering Laboratory. Scientific studies are jointly supported by the U.S. National Science Foundation, New Zealand Foundation for Research, Science and Technology, the Royal Society of New Zealand Marsden Fund, the Italian Antarctic Research Program, the German Science Foundation, and the Alfred-Wegener Institute for Polar and Marine Research. Peter Barrett, Andrew Mackintosh, James Kennett, and Mike Hambrey are thanked for helpful comments on earlier versions of this manuscript. We are grateful to John Anderson, Eugene Domack, and Chris Fielding for their constructive reviews of the submitted manuscript.

APPENDIX. FACIES DESCRIPTIONS

Facies 1: Diatomite

Facies 1 consists of massive to weakly stratified diatomite (e.g., Fig. 8A). Stratification is defined by color changes or laminae/beds of sandstone and gravel. Dispersed pebbles, granules, and coarse sand are common throughout and may deform the laminae beneath. The degree of bioturbation is variable and commonly consists of simple horizontal, millimeter-scale ovoid burrows, although several different types of millimeter- to centimeter-scale trace fossils are present. Microfaulting with millimeter- to centimeter-scale offsets is common throughout, although it is usually more intense in intervals overlain by diamictites (facies 9 and 10). Pure diatomite (e.g., Fig. 8A), which lack a significant terrigenous component but have occasional lonestones, is common, although some intervals consist of up to 50% terrigenous material (e.g., Fig. 5B). Facies 1 represents biopelagic sedimentation, with a variable contribution from hemipelagic deposition in a high-nutrient, marine environment. Periods of iceberg rafting are recorded throughout.

Facies 2: Mudstone

This facies is represented by silty claystones to clayey siltstones (e.g., Fig. 8B) that are predominantly massive in structure. If present, stratification is identified by a change in either color or particle size, and sandstone laminae or thin beds (millimeter to centimeter scale) are present locally. Sandstone laminae and beds are predominantly volcanic in composition, massive or graded, and often display planar or ripple lamination. Bioturbation commonly is absent, although it can be sufficiently intense to obscure primary stratification. Bioturbation usually increases towards contacts with facies 1. Lonestones are largely absent, but they are more common where bioturbation is present. Below 759.32 meters below seafloor (mbsf), bioturbation is absent to extremely rare. However, bioturbation may be present but obscured by a significant dark-colored overprint, attributed to abundant pyrite. A biosiliceous component (e.g., diatom-bearing [10%–25%] to diatom-rich [25%–50%] mudstone) is also common above 586.59 mbsf but rare to absent below this depth. This distribution of biogenic opal may be due, at least in part, to an opal Cristobalite-Tridymite transformation at ~600 mbsf (Scherer et al., 2007).

Facies 2 records environments that were either distal or proximal to grounded ice and were dominated by hemipelagic suspension settling. Greater bioturbation is thought to imply a more distal environment, with slower sedimentation rates, whereas nonbioturbated mudstone may have been deposited in a more proximal grounding line environment. In the lower part of the core (below 759.33 mbsf), the apparent lack of bioturbation in 5- to 10-m-thick mudstones may indicate an environment where sedimentation rates were too high to support a benthic infauna. Alternatively, the heavy pyritization and/or dysaerobic condition in this part of the core may have obscured any bioturbation. The lack of diatoms in these units may also be due to rapid input of terrigenous sediment, which would have restricted primary productivity due to turbidity in the water column.

Where stratified, the siltstone and sandstone laminae may represent a contribution from distal sediment gravity flows, or the winnowing of fines, perhaps related to submarine outwash or bottom currents. This facies may also include a rare ice-rafted component in the form of rare lonestones/pebble nests or poorly sorted coarse sand and diamictite beds.

Facies 3: Interstratified Mudstone and Sandstone

Facies 3 consists of mudstones similar in texture and composition to those of facies 2 but interbedded with graded and massive sandstones on a centimeter- to decimeter-scale (e.g., Fig. 8C). The sandstones are mainly very fine- to medium-grained, but they can reach coarse sand grade. The sandstone beds commonly are graded and are associated with a variety of sedimentary structures, notably planar and ripple lamination. The lower contacts of the sandstones usually are sharp, whereas the upper contacts are gradational (e.g., Fig. 8C). Some sandstone intervals are dominated by volcanic grains, whereas others contain a diverse range of lithologies and minerals. Lonestones of various lithologies are common and occasionally deform underlying laminae. Bioturbation often is present within finer-grained intervals and is also more common near contacts with facies 1.

The fine-grained nature of this facies and the lack of in situ macrofossils or benthic diatoms indicate deposition in a deep-water environment. The interstratified nature is likely the result of hemipelagic sedimentation derived from turbid plumes, which alternated with distal to proximal sediment gravity flows or turbidity currents resulting from grounding line processes or volcanic/tectonic activity. Sandstones with a notable quartzo-feldspathic component and containing planar and ripple laminae (e.g., Fig. 9C) suggest the influence of proglacial grounding line fan processes. These types of sandstones commonly occur near other facies interpreted as proglacial (e.g., rhythmically interlaminated mudstone with siltstone/sandstone, stratified diamictites, conglomerates, etc). Ice rafting also may have contributed sand grains and clasts with diverse lithologies. Traction currents represent another process that probably was active during deposition of this facies, either reworking the tops of gravity flow deposits or as separate traction currents.

Facies 4: Mudstone with Dispersed/Common Clasts

Facies 4 consists of mudstones and sandy mudstones with dispersed (trace to <1%) clasts or mudstone with common (1%–5%) clasts. Facies 4 differs from facies 2 (which may also contain rare lonestones) based on the persistence of clasts throughout facies 4, albeit sometimes in very low abundances. Facies 4 is also very similar to the two diamictite lithofacies (facies 9 and 10) but is distinguished by the relative abundance of sand and/or gravel, using the classification scheme of Moncreiff (1989). Clasts are predominantly granules to small pebbles with diverse lithologies. Bioturbation can be pervasive locally, but often is absent. Microfaulting and fracturing are common, particularly where facies 4 underlies diamictite. Stratification, if present, is defined by changes in color and grain size. Diatoms are present in some intervals above the volcanic succession at 759.33–558.75 mbsf (Fig. 2) but are rare to absent below 759.33 mbsf.

The depositional conditions interpreted for facies 4 are similar to those interpreted for facies 2, except that the presence of dispersed to common clasts indicates rainout from floating ice, either beneath an ice shelf or from icebergs. In association with facies 10, intervals of facies 4 that lack bioturbation could indicate deposition beneath grounded ice, although intervals with clast nests record deposition beneath iceberg zones (Powell and Cooper, 2002). The presence of bioturbation suggests a marine environment that was relatively distal from the grounding line. The high mud content is interpreted as representing sedimentation from turbid plumes in a pro–grounding line marine environment, with clasts being contributed from floating ice.

Facies 5: Rhythmically Interlaminated Mudstone with Siltstone or Sandstone

Facies 5 consists of rhythmically interlaminated couplets of either siltstone or very fine-grained sandstone that grade upward into claystone with iceberg-rafted debris (e.g., Fig. 9B). Claystone and siltstone form fining-upward couplets that are bundled into packages 2 to 5 cm thick. Each package contains 6–10 couplets both above and below a claystone-dominated lamina, which itself is up to 2 cm thick. Individual couplets have a basal lamina of clayey siltstone or very fine sandstone, 2 to 5 mm thick, which grades into a 1–2-mm-thick claystone lamina. Thinner couplets appear more discrete and their sandstone-siltstone laminae are well-sorted. Thicker couplets are less well-defined, contain more mudstone, and their sandstone/siltstone is less well sorted. Couplet thicknesses vary systematically within each package, producing a strong rhythmicity. Mudstone laminae can be present within the sandstone in the coarser part of a couplet. Facies 5 also contains lonestones, which have formed impact structures in the underlying laminae, clast nests, and lenses and beds of poorly sorted, medium to coarse sandstone and granules (Fig. 9A).

Facies similar to our facies 5 have been described from modern temperate to subpolar glacimarine environments in Alaska and the Greenland margin (Table 1), where they are deposited in quiet-water basins by suspension settling from meltwater plumes (Mackiewiez et al., 1984; Cowan et al., 1999; Ó Cofaigh and Dowdeswell, 2001). We infer a similar origin for this facies in AND-1B. These couplets are termed cyclopsams (sandstone/mudstone) for the coarser, more ice-proximal deposits and cyclopels (siltstone/mudstone) for the finer, ice-distal equivalents. The rhythmicity likely resulted from turbid meltwater plumes interacting with tidal currents near the top of the water column. This interaction modulated the settling of suspended sediment to the seafloor (Cowan et al., 1999).

Facies 6: Sandstone

Facies 6 is composed of interbedded siltstone, muddy sandstone, and very fine- to coarse-grained sandstone. The beds predominantly are volcanic-rich and black in color, and they occasionally contain mud rip-up clasts. Normal grading is common, although some massive beds are present. Planar lamination is the most common stratification type, with rare cases of

cross-stratification present. Reverse-graded sandstone beds are also present, but they are less common than normal-graded beds. Bed bases usually are sharp and irregular, whereas tops are either gradational or sharp and planar. Soft-sediment deformation structures are common locally. The sandstones are often interbedded with sandy mudstones or siltstones, which are either massive or laminated.

This facies is interpreted as turbidites, usually with incomplete Bouma sequences (Bouma, 1962). Beds grading upward from Ta (massive sandstone) and Tb (planar laminated sandstone) intervals, before passing directly into Te (massive mudstone) intervals are common. Though complete Bouma sequences from Ta to Te divisions do occur, they generally are rare. The incomplete sequences are interpreted as fines-depleted, proximal turbidites. Because these beds generally are volcanic-rich, the turbidity flows that deposited them may have been triggered by coseismic activity related to volcanism.

Facies 7: Conglomerate

Facies 7 is composed of matrix- to clast-supported sandy muddy conglomerate (e.g., Fig. 9D), usually with rounded to subrounded clasts of diverse lithologies. The conglomerates often are weakly stratified and are generally are <2 m thick. Rarely, conglomerates are composed of >90% elongate mudstone intraclasts, with horizontally aligned long (*a*-) axes. Basal contacts of the conglomerate beds are sharp and irregular, and generally have relief of ~1 cm. Where associated with facies 4, 9, or 10, the contacts are often gradational. Facies 7 is uncommon within the core, and it likely records episodes of submarine sediment redeposition, possibly during turbulent discharge from subglacial conduits.

Facies 8: Breccia

Facies 8 is composed of poorly sorted breccias of sand, granule, and gravel clasts in a muddy or sandy matrix. The clasts are dominated by angular to subrounded granules and pebbles of volcanic origin and/or mud intraclasts. The lower contacts of the breccias generally are sharp and irregular and vary from horizontal to inclined (<30°). These breccias are interpreted to have formed by sediment redeposition by submarine mass-flow processes, mainly from a volcanic source.

Facies 9: Stratified Diamictite

Facies 9 is represented by clast-rich to clast-poor diamictite. Stratification ranges from weak to well-defined and is identified by changes in color, clast concentration, and/or particle size (e.g., Fig. 7A). Horizontal alignment of clasts is not used as a criterion for stratification, although preferred *a*-axis orientation is common. The matrix ranges from muddy to sandy, and the biogenic silica content is variable, ranging from absent to biosiliceous-rich (i.e., up to 50% of the matrix). Clasts are angular to rounded, poorly sorted, and include a wide range of lithologies, such as mudstone intraclasts and volcanics, metasedimentary and sedimentary rocks, granites, dolerites, and marbles. Outsized clasts and pebble nests are present in some intervals (e.g., Figs. 7A and 9A). Facies 9 is often interbedded with, or grades to, facies 10. Bioturbation is present in some intervals but is rare overall.

The origin of the stratified diamictites is diverse. Thinner beds associated with marine facies (e.g., facies 1) are interpreted to have formed by ice rafting or debris-flow deposition. For stratified diamictites that are associated with ice contact or grounding line proximal facies (e.g., facies 3, 4, and 10), depositional processes may have included rain-out of basal glacial debris and associated reworking by marine outwash, or debris flows coming from the grounding line (Powell, 1990). Alternatively, a stratified diamictite could have been deposited beneath grounded ice. Some of the stratified diamictites are dominated by mudstone intraclasts, which may correspond to the granulated facies of Domack et al. (1999), which was interpreted to represent meltout of basal debris during the initial phase of lift-off of grounded ice. Stratified diamictites were analyzed for grain size by sieve and Sedigraph™, and they show a homogeneous distribution (e.g., Figs. 3–6). They generally lack a well-defined mode, although some display a very broad medium-silt mode. Most stratified diamictites are classified as muddy diamictites, but the clay fraction (>8ø) is highly variable in abundance (ranges from 17% to 74%).

Facies 10: Massive Diamictite

In general, the textural and compositional characteristics of facies 10 are identical to those of the stratified diamictites of facies 9. Although facies 10 is not stratified, alignment of clast *a*-axes is common. Sharp lower contacts are often associated with load features, and fracturing is common. The mud, sand, and clast contents of facies 10 are variable, and the diamictite may be interbedded with, or grade into and out of, facies 4 or 9. Clast roundness is also variable, ranging from angular to rounded. Massive diamictites were analyzed for grain-size distribution through sieve and Sedigraph™ analysis (e.g., Figs. 3–6). They lack any well-defined mode, which is similar to the homogeneous distribution of facies 9 (stratified diamictites). Some display a very broad mode combining the fine sand to fine silt modes, but this is not as common as for facies 9.

This facies is interpreted as most likely recording subglacial (ice contact) deposition, although rainout from floating ice and icebergs, and deposition by mass flows originating from the grounding line cannot be excluded. Although the specific depositional process may not be interpretable for a particular diamictite, the occurrences of facies 10 generally are taken as indicators of ice proximity. Where the basal contact of an interval of facies 10 is sharp and overlies a zone of physical mixing (e.g., Figs. 7B and 8A), that diamictite is interpreted as a till, deposited beneath grounded ice.

Facies 11: Volcanic Rocks and Sediments

This facies consists of primary and near-primary volcanic deposits. It includes abundant volcanic sandstone, rare lapilli tuff, and a basaltic lava flow (646.49 to 649.3 mbsf). With the exception of the lava flow, all deposits of facies 11 have undergone some minor redeposition.

REFERENCES CITED

Alonso, B., Anderson, J.B., Diaz, J.I., and Bartek, L.R., 1992, Pliocene-Pleistocene seismic stratigraphy of the Ross Sea; evidence for multiple ice sheet grounding episodes, *in* Elliot, D.H., ed., Contributions to Antarctic Research III: Antarctic Research Series, v. 57, p. 93–103.

Anderson, J.B., and Ashley, G.M., 1991, Glacial marine sedimentation; paleoclimatic significance; a discussion, *in* Anderson, J.B., and Ashley, G.M., eds., Glacial Marine Sedimentation; Paleoclimatic Significance: Geological Society of America Special Paper 261, p. 223–226.

Anderson, J.B., Kurtz, D.D., Domack, E.W., and Balshaw, K.K., 1980, Glacial and glacial marine sediments of the Antarctic continental shelf: The Journal of Geology, v. 88, p. 399–414.

Ashley, G.M., and Smith, N.D., 2000, Marine sedimentation at a calving glacier margin: Geological Society of America Bulletin, v. 112, p. 657–667, doi: 10.1130/0016-7606(2000)112<0657:MSAACG>2.3.CO;2.

Azetsu-Scott, K., and Syvitski, J.P.M., 1999, Influence of melting icebergs on distribution, characteristics and transport of marine particles in an East Greenland fjord: Journal of Geophysical Research, v. 104, no. C3, p. 5321–5328, doi: 10.1029/1998JC900083.

Barker, P.F., Camerlenghi, A., Acton, G.D., Brachfeld, S.A., Cowan, E.A., Daniels, J., Domack, E.W., Escutia, C., Evans, A.J., Eyles, N., Guyodo, Y.J.B., Iorio, M., Iwai, M., Kyte, F.T., Lauer, C., Maldonado, A., Moerz, T., Osterman, L.E., Pudsey, C.J., Schuffert, J.D., Sjunneskog, C.M., Vigar, K.L., Weinheimer, A.L., Williams, T., Winter, D.M., Wolf-Welling, T.C.W., Nessler, S., and Stokking, L., 1999, Proceedings of the Ocean Drilling Program: Initial Reports, Volume 178: College Station, Texas, Ocean Drilling Program, 60 p.

Barrett, P.J., ed., 1989, Antarctic Cenozoic History from CIROS-1 Drillhole, McMurdo Sound: Department of Scientific and Industrial Research (DSIR) Bulletin, v. 245, 251 p.

Barrett, P.J., 2007, Cenozoic climate and sea level history from glacimarine strata off the Victoria Land coast, Cape Roberts Project, Antarctica, *in* Hambrey, M., Christoffersen, P., Glasser, N., and Hubbard, B., eds., Glacial processes and products: International Association of Sedimentologists Special Publication 39, p. 259–287.

Barrett, P.J., and Hambrey, M.J., 1992, Plio-Pleistocene sedimentation in Ferrar Fiord, Antarctica: Sedimentology, v. 39, p. 109–123, doi: 10.1111/j.1365-3091.1992.tb01025.x.

Barrett, P.J., Carter, L., Dunbar, G.B., Dunker, E., Giorgetti, G., Harper, M.A., McKay, R.M., Niessen, F., Nixdorf, U., Pyne, A.R., Riesselmann, C., Robinson, N., Hollis, C., and Strong, P., 2005, Oceanography and Sedimentation beneath the McMurdo Ice Shelf in Windless Bight, Antarctica: Wellington, Antarctic Research Centre, Victoria University of Wellington, Antarctic Data Series, v. 25, 100 p.

Barron, J., Larsen, B., and Shipboard Scientific Party, 1989, Proceedings of the Ocean Drilling Project, Initial Reports, Volume 119: College Station, Texas, Ocean Drilling Program, 942 p.

Bart, P.J., 2001, Did the Antarctic ice sheets expand during the early Pliocene?: Geology, v. 29, p. 67–70, doi: 10.1130/0091-7613(2001)029<0067:DTAISE>2.0.CO;2.

Bart, P.J., 2003, Were West Antarctic Ice Sheet grounding events in the Ross Sea a consequence of East Antarctic Ice Sheet expansion during the middle Miocene?: Earth and Planetary Science Letters, v. 216, p. 93–107, doi: 10.1016/S0012-821X(03)00509-0.

Bart, P.J., Anderson, J.B., Trincardi, F., and Shipp, S.S., 2000, Seismic data from the Northern Basin, Ross Sea, record extreme expansions of the East Antarctic Ice Sheet during the late Neogene: Marine Geology, v. 166, p. 31–50, doi: 10.1016/S0025-3227(00)00006-2.

Bartek, L.R., and Anderson, J.B., 1992, Facies distribution resulting from sedimentation under polar interglacial climatic conditions within a high-latitude marginal basin, McMurdo Sound, Antarctica, *in* Anderson, J.B., and Gail, A.G., eds., Glacial Marine Sedimentation: Paleoclimatic Significance: Geological Society of America Special Paper 261, p. 27–49.

Bouma, A.H., 1962, Sedimentology of Some Flysch Deposits: A Graphic Approach to Facies Interpretation: Amsterdam, Elsevier, 168 p.

Brancolini, G., Cooper, A.K., and Coren, F., 1995, Seismic facies and glacial history in the western Ross Sea (Antarctica), *in* Cooper, A.K., Barker, P.F., and Brancolini, G., eds., Geology and Seismic Stratigraphy of the Antarctic Margin: American Geophysical Union Antarctic Research Series, v. 68, p. 209–234.

Carter, L., Mitchell, J.S., and Day, N.J., 1981, Suspended sediment beneath permanent and seasonal ice, Ross Ice Shelf, Antarctica: New Zealand Journal of Geology and Geophysics, v. 24, p. 249–262.

Carter, L., Dunbar, G., McKay, R., and Naish, T., 2007, Sedimentation and oceanography beneath the McMurdo Ice Shelf at Windless Bight: Wellington, Antarctic Research Centre, Victoria University of Wellington, Antarctic Data Series v. 32, 31 p.

Conway, H., Hall, B.L., Denton, G.H., Gades, A.M., and Waddington, E.D., 1999, Past and future grounding-line retreat of the West Antarctic Ice Sheet: Science, v. 286, no. 5438, p. 280–283, doi: 10.1126/science.286.5438.280.

Cooper, A.K., Davey, F.J., and Behrendt, J.C., 1987, Seismic stratigraphy and structure of the Victoria Land Basin, western Ross Sea, Antarctica, *in* Cooper, A.K., and Davey, F.J., eds., The Antarctic Continental Margin: Geology and Geophysics of the Western Ross Sea: Houston, Texas, Circum-Pacific Council for Energy and Mineral Resources, Earth Science Series, p. 93–118.

Cooper, A.F., Adam, L.J., Coulter, R.F., Eby, G.N., and McIntosh, W.C., 2007, Geology, geochronology and geochemistry of a basanitic volcano, White Island, Ross Sea, Antarctica: Journal of Volcanology and Geothermal Research, v. 165, p. 189–216, doi: 10.1016/j.jvolgeores.2007.06.003.

Cowan, E.A., and Powell, R.D., 1991, Ice-proximal sediment accumulation rates in a temperate glacial fjord, southeastern Alaska, *in* Anderson, J.B., and Ashley, G.M., eds., Glacial Marine Sedimentation; Paleoclimatic Significance: Geological Society of America, Special Paper 261, p. 61–73.

Cowan, E.A., Jinkui, C., Powell, R.D., Clark, J.D., and Pitcher, J.N., 1997, Temperate glacimarine varves: An example from Disenchantment Bay, southern Alaska: Journal of Sedimentary Research, v. 67, p. 536–549.

Cowan, E.A., Seramur, K.C., Cai, J., and Powell, R.D., 1999, Cyclic sedimentation produced by fluctuations in meltwater discharge, tides and marine productivity in an Alaskan fjord: Sedimentology, v. 46, p. 1109–1126, doi: 10.1046/j.1365-3091.1999.00267.x.

Crowley, T.J., Poore, R.Z., and Sloan, L.C., 1996, Pliocene climates; the nature of the problem. Climates and climate variability of the Pliocene: Marine Micropaleontology, v. 27, no. 1–4, p. 3–12, doi: 10.1016/0377-8398(95)00049-6.

Dawber, M., and Powell, R.D., 1997, Epifaunal distributions at Antarctic marine-ending glaciers; influences of ice dynamics and sedimentation, *in* Ricci, C.A., ed., The Antarctic Region; Geological Evolution and Processes: Proceedings of the VII International Symposium on Antarctic Earth Sciences, Siena, Italy: Siena, Italy, Terra Antartica Publications, p. 875–884.

Denton, G.H., and Hughes, T.J., 2000, Reconstruction of the Ross Ice drainage system, Antarctica, at the Last Glacial Maximum: Geografiska Annaler, Series A, Physical Geography, v. 82, p. 143–166, doi: 10.1111/j.0435-3676.2000.00120.x.

Denton, G.H., and Hughes, T.J., 2002, Reconstructing the Antarctic Ice Sheet at the Last Glacial Maximum: Quaternary Science Reviews, v. 21, p. 193–202, doi: 10.1016/S0277-3791(01)00090-7.

De Santis, L., Anderson, J.B., Brancolini, G., and Zayatz, I., 1995, Seismic record of late Oligocene through Miocene glaciation on the central and eastern continental shelf of the Ross Sea, *in* Cooper, A.K., et al., eds., Geology and Seismic Stratigraphy of the Antarctic Margin: American Geophysical Union Antarctic Research Series, v. 68, p. 235–260.

De Santis, L., Prato, S., Brancolini, G., Lovo, M., and Torelli, L., 1999, The eastern Ross Sea continental shelf during the Cenozoic and implications for the West Antarctic Ice Sheet development: Global and Planetary Change, v. 23, p. 173–196, doi: 10.1016/S0921-8181(99)00056-9.

Desloges, J.R., Gilbert, R., Nielsen, N., Christiansen, C., Rasch, M., and Øhlenschlager, R., 2002, Holocene glacimarine sedimentary environments in fiords of Disko Bugt and West Greenland: Quaternary Science Reviews and Research, v. 21, p. 947–963, doi: 10.1016/S0277-3791(01)00049-X.

Domack, E.W., and Ishman, S.E., 1993, Oceanographic and physiographic controls on modern sedimentation within Antarctic fjords: Geological Society of America Bulletin, v. 105, p. 1175–1189, doi: 10.1130/0016-7606(1993)105<1175:OAPCOM>2.3.CO;2.

Domack, E.W., and Williams, C.R., 1990, Fine structure and suspended sediment transport in three Antarctic fjords: Contributions to Antarctic Research, v. 50, p. 71–89.

Domack, E.W., Jacobson, E.A., Shipp, S., and Anderson, J.B., 1999, Late Pleistocene–Holocene retreat of the West Antarctic Ice-Sheet system in the Ross Sea: Part 2. Sedimentologic and stratigraphic signature: Geological Society of America Bulletin, v. 111, no. 10, p. 1517–1536, doi: 10.1130/0016-7606(1999)111<1517:LPHROT>2.3.CO;2.

Domack, E.W., Leventer, A., Dunbar, R., Taylor, F., Brachfeld, S., Sjunneskog C., and ODP Leg 178 Scientific Party, 2001, Chronology of the Palmer Deep site, Antarctic Peninsula: A Holocene palaeoenvironmental reference for the circum-Antarctic: The Holocene, v. 11, p. 1–9, doi: 10.1191/095968301673881493.

Domack, E., Duran, D., Leventer, A., Ishman, S., Doane, S., McCallum, S., Amblas, D., Ring, J., Gilbert, R., and Prentice, M., 2005, Stability of the Larsen B ice shelf on the Antarctic Peninsula during the Holocene epoch: Nature, v. 436, no. 7051, p. 681–685, doi: 10.1038/nature03908.

Dowdeswell, J.A., and Dowdeswell, E.K., 1989, Debris in icebergs and rates of glacimarine sedimentation: Observations from Spitsbergen and a simple model: The Journal of Geology, v. 97, p. 221–231.

Dowdeswell, J.A., Whittington, R.J., and Marienfeld, P., 1994, The origin of massive diamicton facies by iceberg rafting and scouring, Scoresby Sund, East Greenland: Sedimentology, v. 41, p. 21–35, doi: 10.1111/j.1365-3091.1994.tb01390.x.

Dowdeswell, J.A., Elverhøi, A., and Spielhagen, R., 1998, Glacimarine sedimentary processes and facies on the Polar North Atlantic margins: Quaternary Science Reviews, v. 17, p. 243–272, doi: 10.1016/S0277-3791(97)00071-1.

Dunbar, R.B., Leventer, A.R., and Stockton, W.L., 1989, Biogenic sedimentation in McMurdo Sound, Antarctica: Marine Geology, v. 85, p. 155–179, doi: 10.1016/0025-3227(89)90152-7.

Elverhøi, A., Liestøl, O., and Nagy, J., 1980, Glacial erosion, sedimentation and microfauna in the inner part of Kongsfjorden, Spitsbergen: Norsk Polarinstitutt Skrifter, v. 172, p. 33–58.

Elverhøi, A., Lønne, O., and Seland, R., 1983, Glaciomarine sedimentation in a modern fjord environment, Spitsbergen: Polar Research, v. 1, p. 127–149, doi: 10.1111/j.1751-8369.1983.tb00697.x.

Esser, R.P., Kyle, P.R., and McIntosh, W.C., 2004, $^{40}Ar/^{39}Ar$ dating of the eruptive history of Mount Erebus, Antarctica: Volcano evolution: Bulletin of Volcanology, v. 66, p. 671–686, doi: 10.1007/s00445-004-0354-x.

Evans, J., Dowdeswell, J.A., Grobe, H., Niessen, F., Stein, R., Hubberten, H.W., and Whittington, R.J., 2002, Late Quaternary sedimentation in Kejser Franz Joseph Fjord and the continental margin of East Greenland, *in* Dowdeswell, J.A., and Ó Cofaigh, C., eds., Glacier-Influenced Sedimentation on High-Latitude Continental Margins: Geological Society of London Special Publication 203, p. 149–179.

Fahnestock, M.A., Scambos, T.A., Bindschadler, R.A., and Kvaran, G., 2000, A millennium of variable ice flow recorded by the Ross Ice Shelf, Antarctica: Journal of Glaciology, v. 46, p. 652–664, doi: 10.3189/172756500781832693.

Fielding, C.F., Naish, T.R., Woolfe, K.J., and Levelle, M.A., 2000, Facies analysis and sequence stratigraphy of CRP-2/2A, Victoria Land Basin, Antarctica: Terra Antartica, v. 7, p. 323–338.

Fricker, H.A., Scambos, T., Bindschadler, R., and Padman, L., 2007, An active subglacial water system in West Antarctica mapped from space: Science, v. 315, p. 1544–1548, doi: 10.1126/science.1136897.

Hall, B.L., Denton, G.H., Hendy, C.H., Denton, G.H., and Hall, B.L., 2000, Evidence from Taylor Valley for a grounded ice sheet in the Ross Sea, Antarctica: Geografiska Annaler–Physical Geography, v. 82, p. 275–303.

Hambrey, M.J., and McKelvey, B., 2000, Neogene fjordal sedimentation on the western margin of the Lambert graben, East Antarctica: Sedimentology, v. 47, p. 577–607, doi: 10.1046/j.1365-3091.2000.00308.x.

Hart, J.K., 1995, Subglacial erosion, deposition and deformation associated with deformable beds: Progress in Physical Geography, v. 19, p. 173–191, doi: 10.1177/030913339501900202.

Hart, J.K., and Boulton, G.S., 1991, The interrelation of glaciotectonic and glaciodepositional processes within the glacial environment: Quaternary Science Reviews, v. 10, p. 335–350, doi: 10.1016/0277-3791(91)90035-S.

Hayes, D.E., Frakes, L.A., Barrett, P.J., Burns, D.A., Chen, P.-H., Ford, A.B., Kaneps, A.G., Kemp, E.M., McCollum, D.W., Piper, D.J.W., Wall, R.E., and Webb, P.N., 1975, Initial Reports of the Deep Sea Drilling Project, Volume 28: Washington, D.C., Government Printing Office, 1017 p., doi: 10.2973/dsdp.proc.28.1975.

Henrys, S.A., Wilson, T.J., Whittaker, J., Fielding, C.R., Hall, J., and Naish, T.R., 2007, Tectonic history of mid-Miocene to Present Southern Victoria Land Basin, inferred from seismic stratigraphy in McMurdo Sound, Antarctica, *in* Cooper, A.K., and Raymond, C.R., eds., Antarctica: A Keystone in a Changing World—Online Proceedings for the Tenth International Symposium on Antarctic Earth Sciences: USGS Open-File Report 2007–1047, Short Research Paper 049, 4 p.

Horgan, H., Naish, T., Bannister, S., Balfour, N., and Wilson, G.S., 2005, Seismic stratigraphy of the Plio-Pleistocene Ross Island flexural moat-fill; a prognosis for ANDRILL Program drilling beneath McMurdo-Ross Ice Shelf: Global and Planetary Change, v. 45, p. 83–97, doi: 10.1016/j.gloplacha.2004.09.014.

Hughes, T., 1977, West Antarctic ice streams: Reviews of Geophysics and Space Physics, v. 15, p. 1–46, doi: 10.1029/RG015i001p00001.

IPCC (Intergovernmental Panel on Climate Change), 2007, Climate Change 2007: The Physical Science Basis. Contribution of Working Group I to the Fourth Assessment Report of the Intergovernmental Panel on Climate Change: Cambridge, UK, Cambridge University Press, 996 p.

Kennett, J.P., and Hodell, D.A., 1993, Evidence for relative climatic stability of Antarctica during the early Pliocene; a marine perspective: Geografiska Annaler, Series A, Physical Geography, v. 75, p. 205–220, doi: 10.2307/521201.

Krissek, L.A., Browne, G.H., Carter, L., Cowan, E.A., Dunbar, G.B., McKay, R.M., Naish, T., Powell, R., Reed, J., Wilch, T.I., and the Andrill MIS Science Team, 2007, Sedimentology and Stratigraphy of the AND-1B Core, ANDRILL McMurdo Ice Shelf Project, Antarctica: Terra Antartica, v. 14, p. 185–222.

Kyle, P.R., 1981, Mineralogy and geochemistry of a basanite to phonolite sequence at Hut Point Peninsula, Antarctica, based on core from Dry Valley Drilling Project Drillholes 1, 2 and 3: Journal of Petrology, v. 22, p. 451–500.

Leckie, R.M., and Webb, P.-N., 1983, Late Oligocene–early Miocene glacial record of the Ross Sea, Antarctica: Evidence from DSDP Site 270: Geology, v. 11, p. 578–582, doi: 10.1130/0091-7613(1983)11<578:LOMGRO>2.0.CO;2.

Lewis, A.R., Marchant, D.R., Kowalewski, D.E., Baldwin, S.L., and Webb, L.E., 2006, The age and origin of the Labyrinth, Western Dry Valleys, Antarctica: Evidence for extensive middle Miocene subglacial floods and freshwater discharge to the Southern Ocean: Geology, v. 34, p. 513–516, doi: 10.1130/G22145.1.

Lewis, A.R., Marchant, D.R., Ashworth, A.C., Hemming, S.R., and Machlus, M.L., 2007, Major middle Miocene global climate change: Evidence from East Antarctica and the Transantarctic Mountains: Geological Society of America Bulletin, v. 119, p. 1449–1461.

Licht, K.J., Dunbar, N.W., Andrews, J.T., and Jennings, A.E., 1999, Distinguishing subglacial till and glacial marine diamictons in the western Ross Sea, Antarctica; implications for a Last Glacial Maximum grounding line: Geological Society of America Bulletin, v. 111, p. 91–103, doi: 10.1130/0016-7606(1999)111<0091:DSTAGM>2.3.CO;2.

Licht, K.J., Lederer, J.R., and Swope, J., 2005, Provenance of LGM glacial till (sand fraction) across the Ross Embayment, Antarctica: Quaternary

Science Reviews, v. 24, p. 1499–1520, doi: 10.1016/j.quascirev.2004.10.017.

Lowe, A.L., and Anderson, J.B., 2002, Reconstruction of the West Antarctic Ice Sheet in Pine Island Bay during the Last Glacial Maximum and its subsequent retreat history: Quaternary Science Reviews, v. 21, p. 1879–1897, doi: 10.1016/S0277-3791(02)00006-9.

MacAyeal, D.R., 1992, Irregular oscillation of the West Antarctic Ice Sheet: Nature, v. 359, p. 29–32, doi: 10.1038/359029a0.

Mackiewicz, N.E., Powell, R.D., Carlson, P.R., and Molnia, B.F., 1984, Interlaminated ice-proximal glacimarine sediments in Muir Inlet, Alaska: Marine Geology, v. 57, p. 113–147, doi: 10.1016/0025-3227(84)90197-X.

MacPherson, A., 1987, The MacKay Glacier/Granite Harbour Glacial Marine Sedimentation System [Ph.D. thesis]: Wellington, Victoria University of Wellington, 173 p.

Marchant, D.R., Denton, G.H., Swisher, C.C., III, and Potter, N., Jr., 1996, Late Cenozoic Antarctic paleoclimate reconstructed from volcanic ashes in the Dry Valleys region of southern Victoria Land: Geological Society of America Bulletin, v. 108, p. 181–194, doi: 10.1130/0016-7606(1996)108<0181:LCAPRF>2.3.CO;2.

McCrae, I.R., 1984, A summary of glaciological measurements made between 1960 and 1984 on the McMurdo Ice Shelf, Antarctica: Auckland, Department of Theoretical and Applied Mechanics, University of Auckland, School of Engineering Report 360, 92 p.

McKay, R.M., Dunbar, G.B., Naish, T.R., Barrett, P.J., Carter, L., and Harper, M., 2008, Retreat history of the West Antarctic Ice (Sheet) Shelf in Western Ross Sea since the Last Glacial Maximum from deep-basin sediment cores: Palaeogeography, Palaeoclimatology, Palaeoecology, v. 260, p. 168–183, doi: 10.1016/j.palaeo.2007.08.014.

McMullen, K., Domack, E., Leventer, A., Olson, C., Dunbar, R.B., and Brachfeld, S., 2006, Glacial morphology and sediment formation in the Mertz Trough, East Antarctica: Palaeogeography, Palaeoclimatology, Palaeoecology, v. 231, no. 1–2, p. 169–180, doi: 10.1016/j.palaeo.2005.08.004.

Miller, K. G., Wright, J. D., and Fairbanks, R. G., 1991, Unlocking the ice house: Oligocene-Miocene oxygen isotopes, eustasy, and margin erosion: Journal of Geophysical Research, v. 96B, p. 6829–6848.

Mosola, A.B., and Anderson, J.B., 2006, Expansion and rapid retreat of the West Antarctic Ice Sheet in eastern Ross Sea: Possible consequence of over-extended ice streams?: Quaternary Science Reviews, v. 25, p. 2177–2196, doi: 10.1016/j.quascirev.2005.12.013.

Naish, T.R., Woolfe, K.J., Barrett, P.J., Wilson, G.S., Cliff, A., Bohaty, S.M., Bucker, C.J., Claps, M., Davey, F.J., Dunbar, G.B., Dunn, A.G., Fielding, C.R., Florindo, F., Hannah, M.J., Harwood, D.M., Henrys, S.A., Krissek, L.A., Lavelle, M., van der Meer, J.J.M., McIntosh, W.C., Niessen, F., Passchier, S., Powell, R.D., Roberts, A.P., Sagnotti, L., Scherer, R.P., Strong, P.C., Talarico, F., Verosub, K.L., Villa, G., Watkins, D.K., Webb, P.-N., Wonik, T., 2001, Orbitally induced oscillations in the East Antarctic ice sheet at the Oligocene/Miocene boundary: Nature, v. 413, p. 719–723, doi: 10.1038/35099534.

Naish, T.R., Powell, R.D., Barrett, P.J., Levy, R., Henrys, S.A., Wilson, G.S., Krissek, L.A., Niessen, F., Pompilio, M., Scherer, R., Talarico, F., and Pyne, A., 2008, Late Cenozoic climate history of the Ross Embayment from the AND-1B drill hole: Culmination of three decades of Antarctic margin drilling, *in* Cooper, A.K., and Raymond, C.R., eds., Antarctica: A keystone in a Changing World: Proceedings from the 10th ISAES, National Academies Press: U.S. Geological Survey Open-File Report 2007-1047, Short Research Paper 049, 4 p.

Naish, T., Powell, R., Levy, R., Wilson, G., Scherer, R., Talarico, F., Krissek, L., Niessen, F., Pompilio, M., Wilson, T., Carter, L., DeConto, R., Huybers, P., McKay, R., Pollard, D., Ross, J., Winter, D., Barrett, P., Browne, G., Cody, R., Cowan, E., Crampton, J., Dunbar, G., Dunbar, N., Florindo, F., Gebhardt, C., Graham, I., Hannah, M., Hansaraj, D., Harwood, D., Helling, D., Henrys, S., Hinnov, L., Kuhn, G., Kyle, P., Läufer, A., Maffioli, P., Magens, D., Mandernack, K., McIntosh, W., Millan, C., Morin, R., Ohneiser, C., Paulsen, T., Persico, D., Raine, I., Reed, J., Riesselman, C., Sagnotti, L., Schmitt, D., Sjunneskog, C., Strong, P., Taviani, M., Vogel, S., Wilch, T., and Williams, T., 2009, Obliquity-paced Pliocene West Antarctic Ice Sheet oscillations: Nature, v. 458, p. 322–328, doi:10.1038/nature07867.

Ó Cofaigh, C., and Dowdeswell, J.A., 2001, Laminated sediments in glacimarine environments: Diagnostic criteria for their interpretation: Quaternary Science Reviews, v. 20, p. 1411–1436.

Ó Cofaigh, C., Dowdeswell, J.A., and Grobe, H., 2001, Holocene glacimarine sedimentation, inner Scoresby Sund, East Greenland: The influence of fast-flowing ice-sheet outlet glaciers: Marine Geology, v. 175, p. 103–129.

Pollard, D., and DeConto, R.M., 2009, Modelling West Antarctic ice sheet growth and collapse through the past five million years: Nature, v. 458, p. 329–332.

Pompilio, M., Dunbar, N., Gebhardt, A.C., Helling, D., Kuhn, G., Kyle, P., McKay, R., Talarico, F., Tulaczyk, S., Vogel, S., Wilch, T., and the ANDRILL-MIS Science Team, 2007, Petrology and geochemistry of the AND-1B core, ANDRILL McMurdo Ice Shelf Project, Antarctica: Terra Antartica, v. 14, p. 255–288.

Powell, R.D., 1990, Grounding-line fans and their growth to ice-contact deltas, *in* Dowdeswell, J., and Scourse, J., eds., Glacimarine Environments: Processes and Sediments: Geological Society of London Special Publication 53, p. 53–73.

Powell, R.D., and Cooper, J.M., 2002, A glacial sequence stratigraphic model for temperate, glaciated continental shelves, *in* Dowdeswell, J.A., and Ó Cofaigh, C., eds., Glacier-Influenced Sedimentation on High-Latitude Continental Margins: Geological Society of London Special Publication 203, p. 215–244, doi: 10.1144/GSL.SP.2002.203.01.12.

Powell, R.D., and Domack, E.W., 2002, Glacimarine environments, *in* Menzies, J., ed., Modern and Past Glacial Environments: Boston, Butterworth-Heinemann, p. 361–390.

Powell, R.D., and Molnia, B., 1989, Glacimarine sedimentary processes, facies and morphology of the south-southeast Alaska shelf and fjords: Marine Geology, v. 85, p. 359–390, doi: 10.1016/0025-3227(89)90160-6.

Powell, R.D., Dawber, M., McInnes, J.N., and Pyne, A.R., 1996, Observations of the grounding-line area at a floating glacier terminus: Annals of Glaciology, v. 22, p. 217–223.

Quilty, P.G., Lirio, J.M., and Jillett, D., 2000, Stratigraphy of the Pliocene Sørsdal Formation, Marine Plain, Vestfold Hills, East Antarctica: Antarctic Science, v. 12, p. 205–216, doi: 10.1017/S0954102000000262.

Raymo, M.E., 1994, The initiation of Northern Hemisphere glaciation: Annual Review of Earth and Planetary Sciences, v. 22, p. 353–383, doi: 10.1146/annurev.ea.22.050194.002033.

Rignot, E., and Jacobs, S.S., 2002, Rapid bottom melting widespread near Antarctic ice sheet grounding lines: Science, v. 296, p. 2020–2023, doi: 10.1126/science.1070942.

Sandroni, S., and Talarico, F., 2006, Analysis of clast lithologies from CIROS-2 core, New Harbour, Antarctica—Implications for ice flow directions during Plio-Pleistocene: Palaeogeography, Palaeoclimatology, Palaeoecology, v. 231, p. 215–232, doi: 10.1016/j.palaeo.2005.07.031.

Scherer, R.P., Aldahan, A.A., Tulaczyk, S., Possnert, G., Engelhardt, H., and Kamb, B., 1998, Pleistocene collapse of the West Antarctic Ice Sheet: Science, v. 281, p. 82–85, doi: 10.1126/science.281.5373.82.

Scherer, R.P., Sjunneskog, C.M., Iverson, N., and Hooyer, T., 2004, Assessing subglacial processes from diatom fragmentation patterns: Geology, v. 32, p. 557–560, doi: 10.1130/G20423.1.

Scherer, R., Hannah, M., Maffioli, P., Persico, D., Sjunneskog, C., Strong, C.P., Taviani, M., Winter, D., and the ANDRILL-MIS Science Team, 2007, Palaeontologic characterisation and analysis of the AND-1B core, ANDRILL McMurdo Ice Shelf Project, Antarctica: Terra Antartica, v. 14, p. 223–254.

Schoof, C., 2007, Ice sheet grounding line dynamics: Steady states, stability and hysteresis: Journal of Geophysical Research, v. 112, p. F03S28, doi: 10.1029/2006JF000664.

Shipboard Scientific Party, 2001, Leg 188 summary: Prydz Bay—Cooperation Sea, Antarctica, *in* O'Brien, P.E., Cooper, A.K., Richter, C., et al., Proceedings of the Ocean Drilling Project: Initial Reports v. 188: College Station, Texas (Ocean Drilling Program), p. 1–65.

Shipp, S., Anderson, J.B., and Domack, E.W., 1999, Late Pleistocene–Holocene retreat of the West Antarctic ice-sheet system in the Ross Sea: Part 1. Geophysical results: Geological Society of America Bulletin, v. 111, p. 1486–1516, doi: 10.1130/0016-7606(1999)111<1486:LPHROT>2.3.CO;2.

Siegert, M.J., Carter, S., Tabacco, I., Popov, S., and Blankenship, D., 2005, A revised inventory of Antarctic subglacial lakes: Antarctic Science, v. 17, p. 453–460, doi: 10.1017/S0954102005002889.

Sjunneskog, C., and Scherer, R.P., 2005, Mixed diatom assemblages in glacigenic sediment from the central Ross Sea, Antarctica: Palaeogeography, Palaeoclimatology, Palaeoecology, v. 218, p. 287–300, doi: 10.1016/j.palaeo.2004.12.019.

Stern, T.A., Davey, F.J., and Delisle, G., 1991, Lithospheric flexure induced by the load of Ross Archipelago, southern Victoria Land, Antarctica, *in* Thomson, M.R.A., Crame, J.A., and Thomson, J.W., eds., Geological Evolution of Antarctica: Proceedings of the Fifth International Symposium on Antarctic Earth Sciences: Cambridge, UK, Cambridge University Press, p. 323–328.

Sugden, D., and Denton, G., 2004, Cenozoic landscape evolution of the Convoy Range to Mackay Glacier area, Transantarctic Mountains; onshore to offshore synthesis: Geological Society of America Bulletin, v. 116, p. 840–857, doi: 10.1130/B25356.1.

Sugden, D.E., Marchant, D.R., and Denton, G.H., 1993, The case for a stable East Antarctic Ice Sheet: Geografiska Annaler, v. 75, p. 151–353, doi: 10.2307/521199.

Summerfield, M.E., Sugden, D.E., Denton, G.H., Marchant, D.R., Cockburn, H.A.P., and Stuart, M.F., 1999, Cosmogenic isotope data support previous evidence of extremely low rates of denudation in the Dry Valleys region, southern Victoria Land, Antarctica, *in* Smith, B., Whalley, W., and Warke, P., eds., Uplift, Erosion and Stability: Perspectives on Long-Term Landscape Development: Geological Society of London Special Publication 162, p. 255–267.

Syvitski, J.P.M., Andrews, J.T., and Dowdeswell, J.A., 1996, Sediment deposition in an iceberg-dominated glacimarine environment East Greenland: Basin fill implications: Global and Planetary Change, v. 12, p. 251–270, doi: 10.1016/0921-8181(95)00023-2.

Talarico, F.M., and Sandroni, S., 2007, Clast provenance and variability in MIS (AND-1B) core and their implications for the paleoclimatic evolution recorded in the Windless Bight, southern McMurdo Sound area (Antarctica), *in* Cooper, A.K., and Raymond, C.R., eds., Antarctica: A Keystone in a Changing World: Online Proceedings for the Tenth International Symposium on Antarctic Earth Sciences: U.S. Geological Survey Open-File Report 2007–1047, Extended abstract 118.

Thomas, R.H., and Bentley, C.R., 1978, A model for Holocene retreat of the West Antarctic Ice Sheet: Quaternary Research, v. 10, p. 150–170, doi: 10.1016/0033-5894(78)90098-4.

Tulaczyk, S., Kamb, B., Scherer, R.P., and Engelhardt, H.F., 1998, Sedimentary processes at the base of a West Antarctic ice stream: Constraints from textural and compositional properties of subglacial debris: Journal of Sedimentary Research, v. 68, p. 487–496.

Webb, P.N., and Harwood, D.M., 1991, Late Cenozoic glacial history of the Ross Embayment, Antarctica: Quaternary Science Reviews, v. 10, p. 215–223, doi: 10.1016/0277-3791(91)90020-U.

Webb, P.-N., Harwood, D.M., McKelvey, B.C., Mercer, J.H., and Stott, L.D., 1984, Cenozoic marine sedimentation and ice volume variation in the East Antarctic craton: Geology, v. 12, p. 287–291, doi: 10.1130/0091-7613(1984)12<287:CMSAIV>2.0.CO;2.

Weertman, J., 1974, Stability of the junction of an ice sheet and an ice shelf: Journal of Glaciology, v. 13, p. 3–13.

Whitehead, J.M., Harwood, D.M., McKelvey, B.C., Hambrey, M.J., and McMinn, A., 2004, Diatom biostratigraphy of the Cenozoic glaciomarine Pagodroma Group, northern Prince Charles Mountains, East Antarctica: Australian Journal of Earth Sciences, v. 51, no. 4, p. 521–547, doi: 10.1111/j.1400-0952.2004.01072.x.

Wilson, G., Levy, R., Browne, G., Dunbar, N., Florindo, F., Henrys, S., Graham, I., McIntosh, W., McKay, R., Naish, T., Ohneiser, C., Powell, R., Ross, J., Sagnotti, L., Scherer, R., Sjunneskog, C., Strong, C., Taviani, M., Winter, D., and the ANDRILL MIS Science Team, 2007, Preliminary chronostratigraphy of the AND-1B core, ANDRILL McMurdo Ice Shelf Project, Antarctic: Terra Antartica, v. 14, p. 297–316.

Wingham, D.J., Siegert, M.J., Shepherd, A., and Muir, A.S., 2006, Rapid discharge connects Antarctic subglacial lakes: Nature, v. 440, p. 1033–1036, doi: 10.1038/nature04660.

Wright, A.C., and Kyle, P.R., 1990a, Mount Bird, *in* Le Masurier and Thomson, eds., Volcanoes of the Antarctic Plate and Southern Oceans: American Geophysical Union Antarctic Research Series, v. 48, p. 97–98.

Wright, A.C., and Kyle, P.R., 1990b, Mount Terror, *in* Le Masurier and Thomson, eds., Volcanoes of the Antarctic Plate and Southern Oceans: American Geophysical Union Antarctic Research Series, v. 48, p. 99–102.

Zachos, J.C., Pagini, M., Sloan, L., Thomas, E., and Billups, K., 2001, Trends, rhythms, and aberrations in global climate 65 Myr to present: Science, v. 292, p. 686–693, doi: 10.1126/science.1059412.

Manuscript Received 11 September 2008
Revised Manuscript Received 29 January 2009
Manuscript Accepted 5 February 2009

Printed in the USA